

## Phosphine-substituted Fe-Te clusters related to the active site of [FeFe]-H<sub>2</sub>ases

Shuang Lü,<sup>a</sup> Hong-Li huang,<sup>b</sup> Ru-fen Zhang,<sup>b</sup> Chun-lin Ma,<sup>b</sup> Qian-Li Li,<sup>\*b</sup> Jiao He,<sup>c</sup> Jun Yang,<sup>c</sup>  
Ting Li,<sup>c</sup> Yu-Long Li<sup>\*c,d</sup>

<sup>a</sup> School of Pharmacy, Liaocheng University, Liaocheng 252059, P.R. China

<sup>b</sup> Shandong Provincial Key Laboratory of Chemical Energy Storage and Novel Cell  
Technology, College of Chemistry and Chemical Engineering, Liaocheng University,  
Liaocheng, 252059, P. R.China

<sup>c</sup>College of Chemistry and Environmental Engineering, Sichuan University of Science  
& Engineering, Zigong 643000, P.R. China

<sup>d</sup>Chemical Synthesis and Pollution Control Key Laboratory of Sichuan Province, China West  
Normal University, Nanchong 637002, P.R. China

## Contents

Figs. S1-S31. IR and NMR spectra for <b>1-6</b> .	page 2-17
Figs. S32-S35. UV-visible spectra of <b>1-6</b> recorded in CH <sub>2</sub> Cl <sub>2</sub> at 25 °C.	page 18-19
Fig. S36. Dependence of current heights of the reduction events for <b>1</b> and <b>2</b> on the concentration of HOAc in CH <sub>3</sub> CN.	page 20
Figure S37. Molecular structures of the compound <b>B</b>	page 20
Table S1. Crystal data and structure parameters for <b>1-anti</b> , <b>2-anti</b> , <b>2-syn</b> and <b>4-6</b> .	page 21
Tables S2-S7. Selected distance (Å) and angles (°) for <b>1-anti</b> , <b>2-anti</b> , <b>2-syn</b> and <b>4-6</b> .	page 22-25

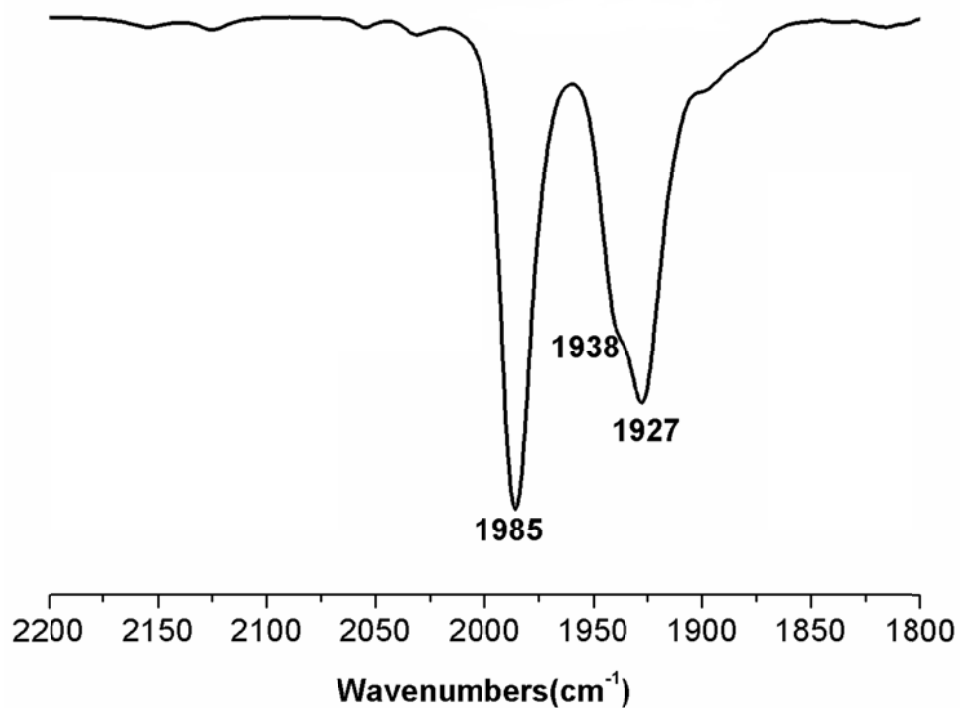


Figure S1. FT-IR (in CH<sub>2</sub>Cl<sub>2</sub>, 25°C) spectrum of **1-anti**. Assignments:  $\nu_{CO} = 1985$ , 1938, 1927 cm<sup>-1</sup>.

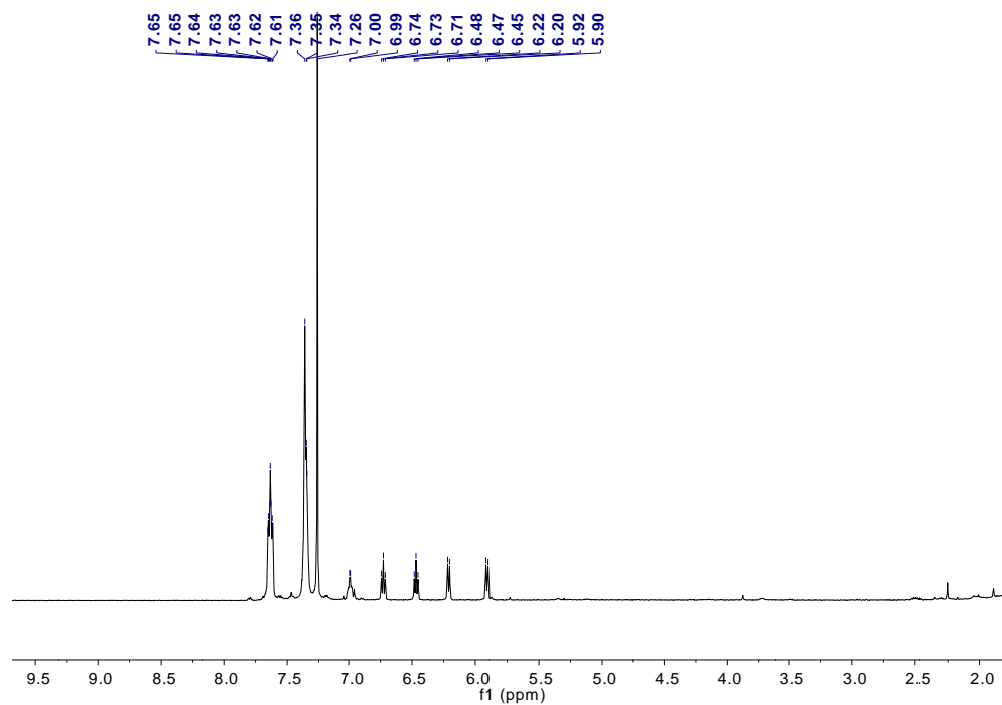


Figure S2. <sup>1</sup>H NMR (500 MHz, CDCl<sub>3</sub>, 25 °C) spectrum of **1-anti**. Assignments:  $\delta = 7.65\text{-}5.90$  (m, 40H, 8C<sub>6</sub>H<sub>5</sub>) ppm.

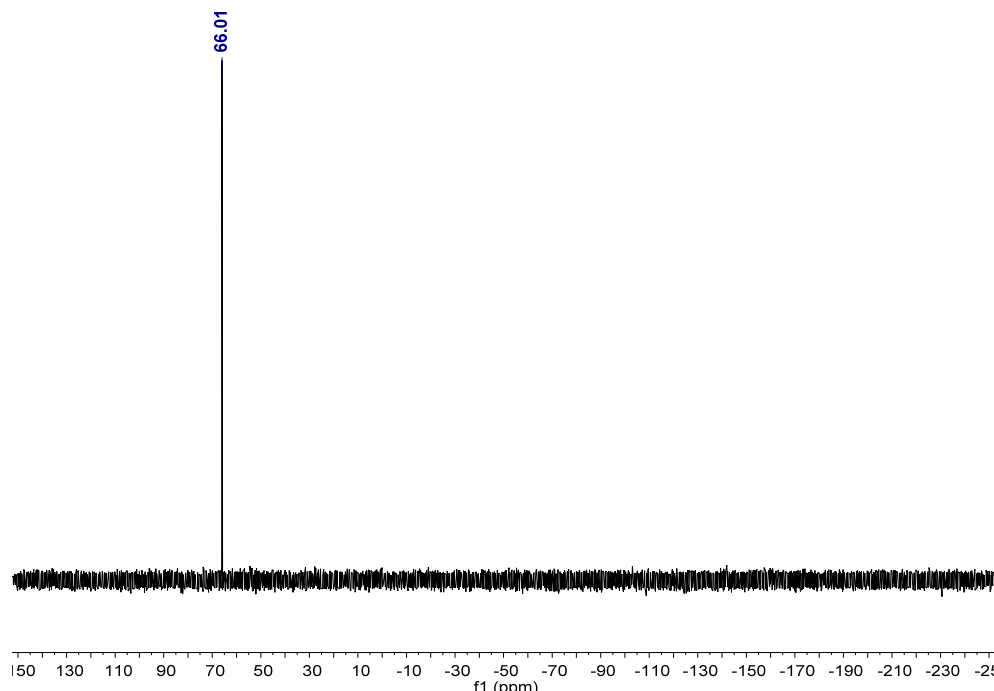


Figure S3.  $^{31}\text{P}$  NMR (202 MHz,  $\text{CDCl}_3$ , 25 °C) spectrum of **1-anti**. Assignments:  $\delta = 66.01$  ppm.

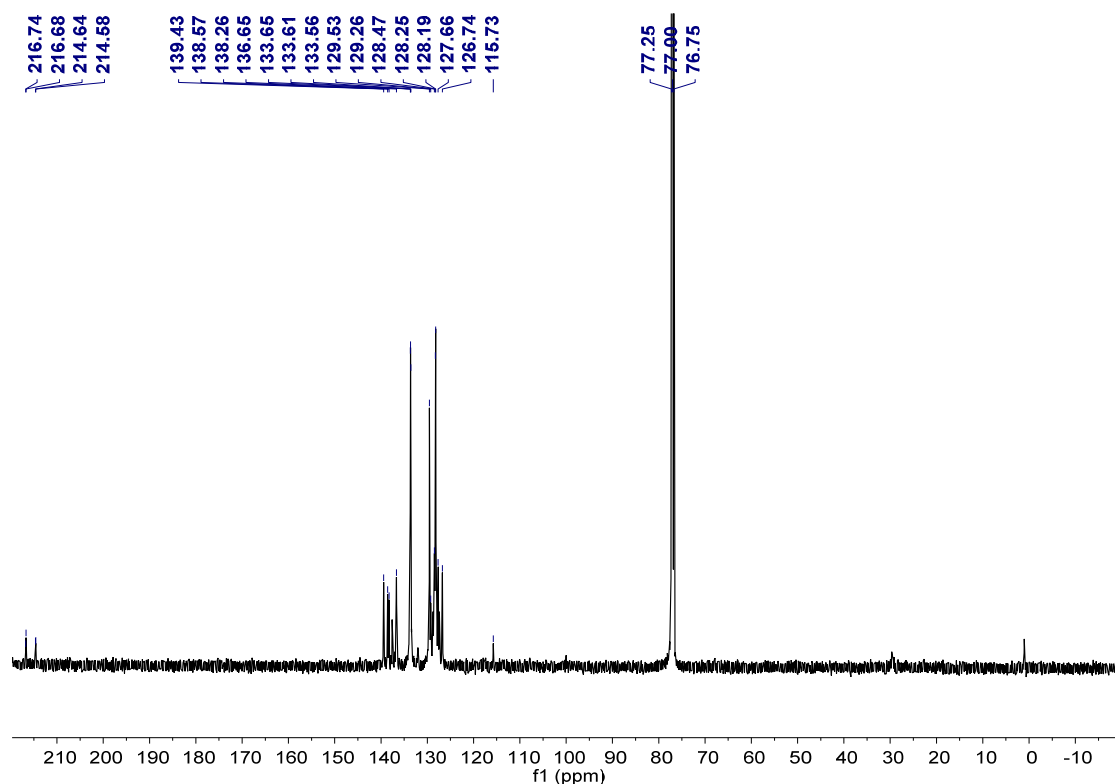


Figure S4.  $^{13}\text{C}$  NMR (126 MHz,  $\text{CDCl}_3$ , 25 °C) spectrum of **1-anti**. Assignments:  $\delta = 216.7, 214.6$  (2d,  $^2J_{\text{P-C}} = 7.6$  Hz,  $\text{PFe}(\text{CO})_2$ ), 115.7-139.4 (m,  $\text{C}_6\text{H}_5$ ) ppm.

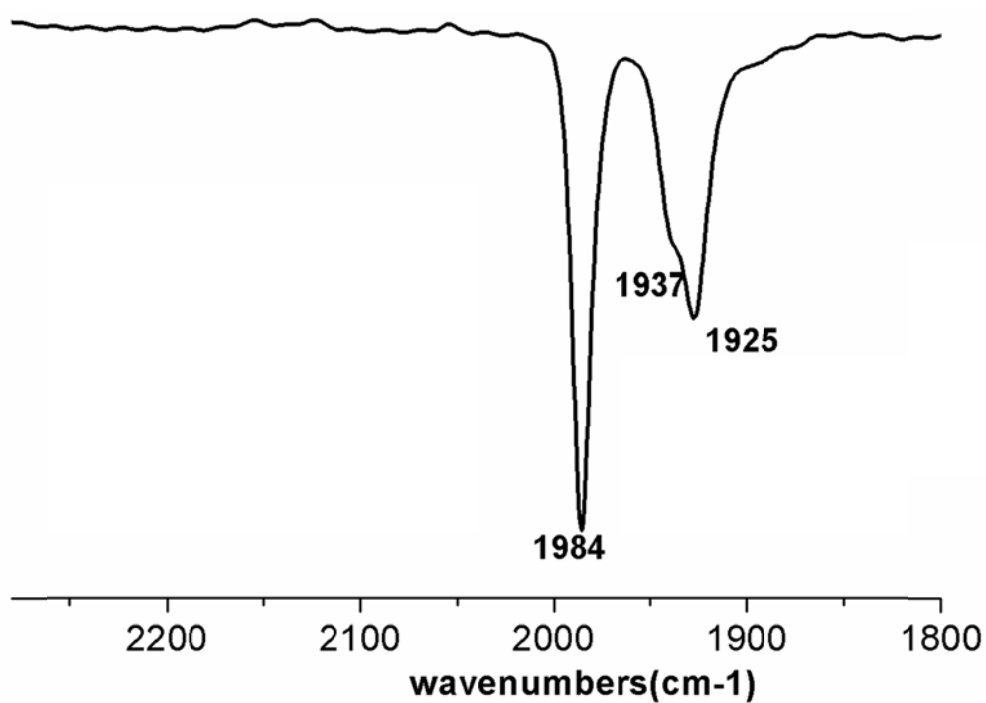


Figure S5. FT-IR (in CH<sub>2</sub>Cl<sub>2</sub>, 25°C) spectrum of **1-syn**. Assignments:  $\nu_{CO} = 1984$ , 1937, 1925 cm<sup>-1</sup>.

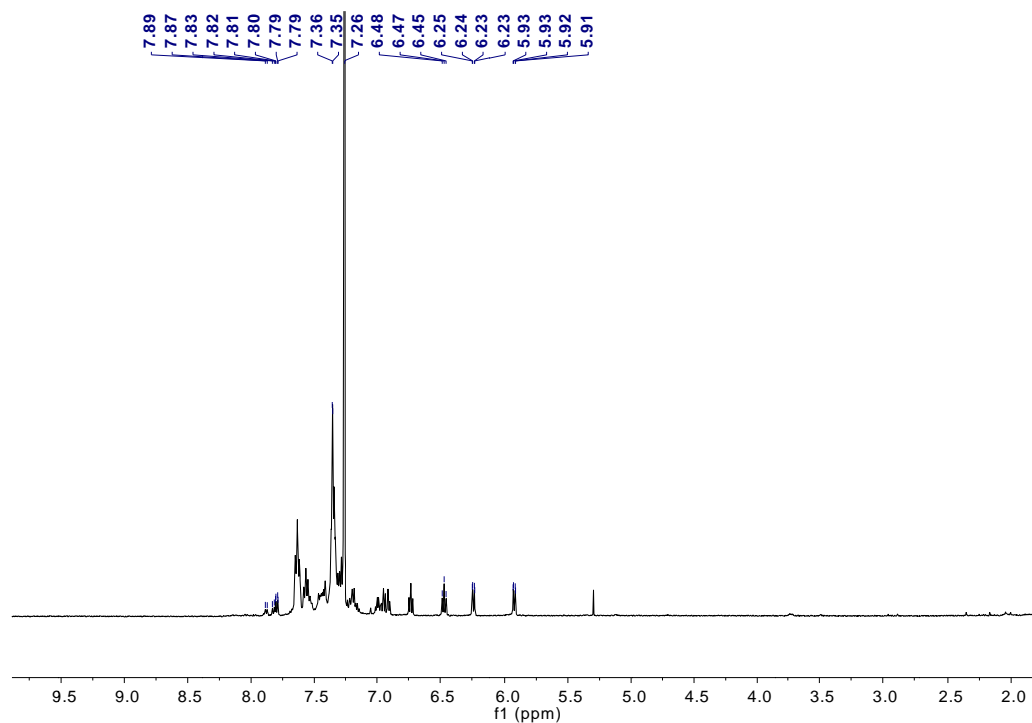


Figure S6. <sup>1</sup>H NMR (500 MHz, CDCl<sub>3</sub>, 25 °C) spectrum of **1-syn**. Assignments:  $\delta = 7.89\text{-}5.91$  (m, 40H, 8C<sub>6</sub>H<sub>5</sub>) ppm.

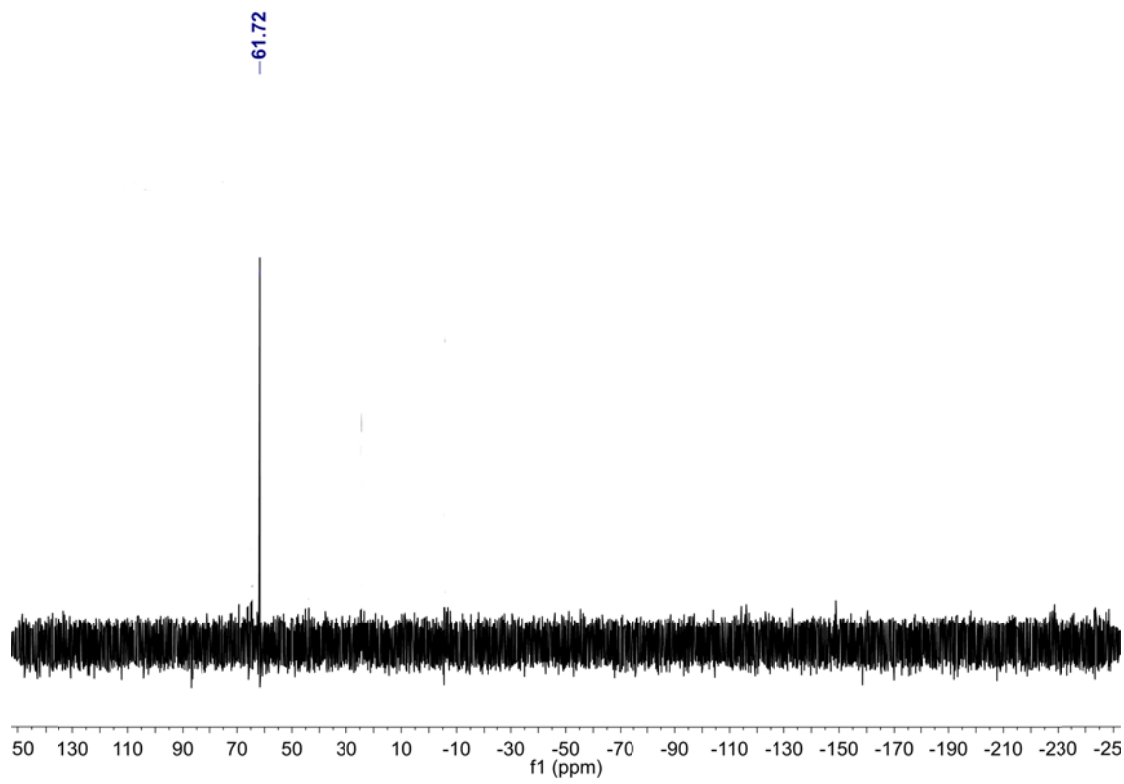


Figure S7.  $^{31}\text{P}$  NMR (202 MHz,  $\text{CDCl}_3$ , 25 °C) spectrum of **1-syn**. Assignments:  $\delta = 61.72$  ppm.

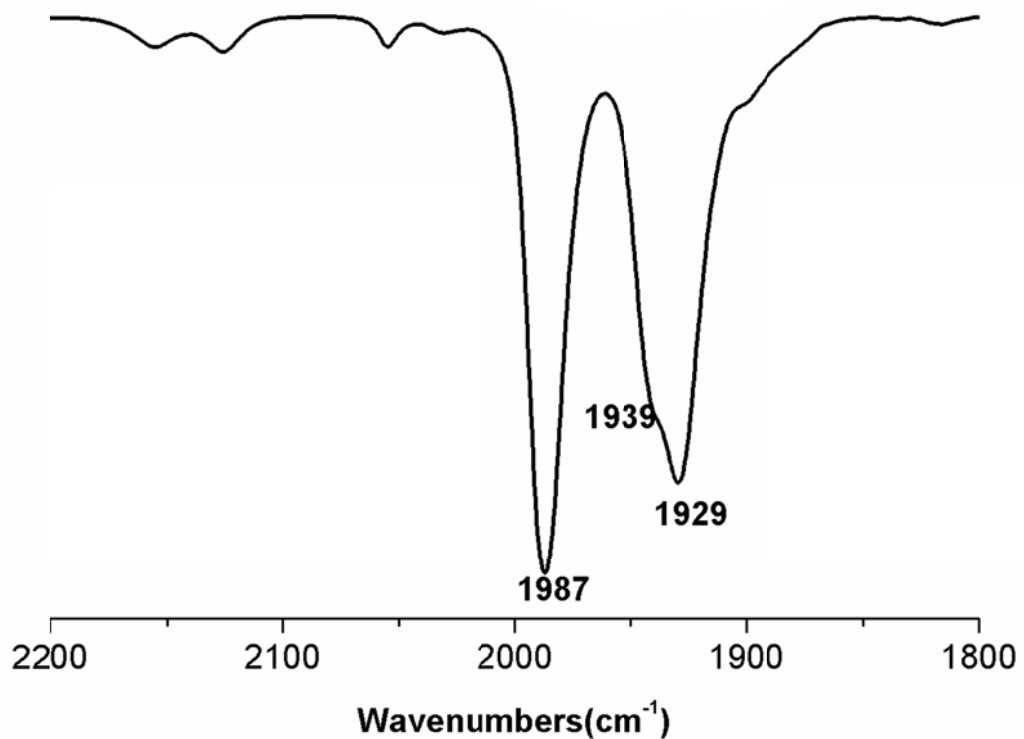


Figure S8. FT-IR (in  $\text{CH}_2\text{Cl}_2$ , 25°C) spectrum of **2-anti**. Assignments:  $\nu_{\text{CO}} = 1987$ , 1939, 1929  $\text{cm}^{-1}$ .

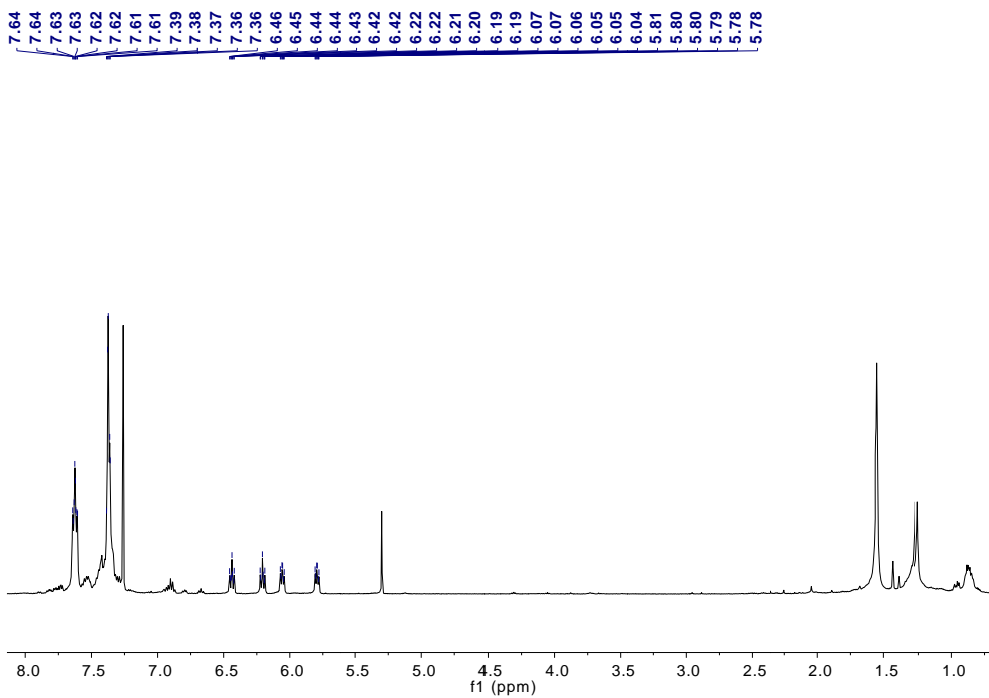


Figure S9.  $^1\text{H}$  NMR (500 MHz,  $\text{CDCl}_3$ , 25 °C) spectrum of **2-anti**. Assignments:  $\delta$  = 7.64–5.78 (m, 38H,  $6\text{C}_6\text{H}_5 + 2\text{C}_6\text{H}_4$ ) ppm.

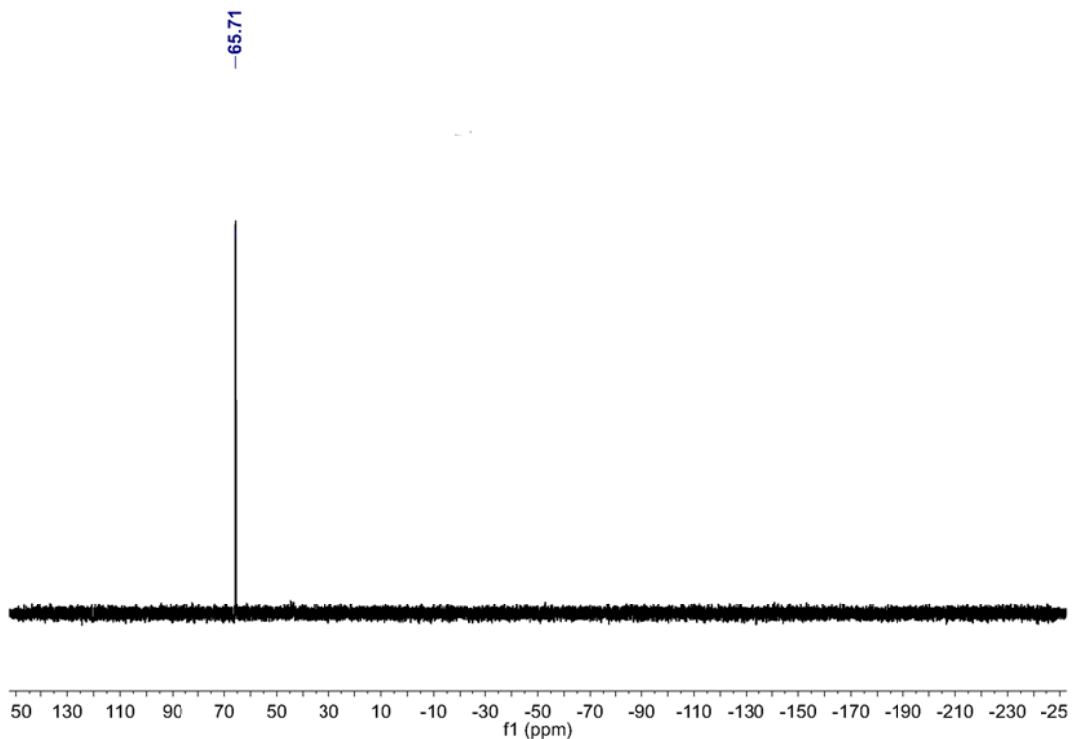


Figure S10.  $^{31}\text{P}$  NMR (202 MHz,  $\text{CDCl}_3$ , 25 °C) spectrum of **2-anti**. Assignments:  $\delta$  = 65.71 ppm.

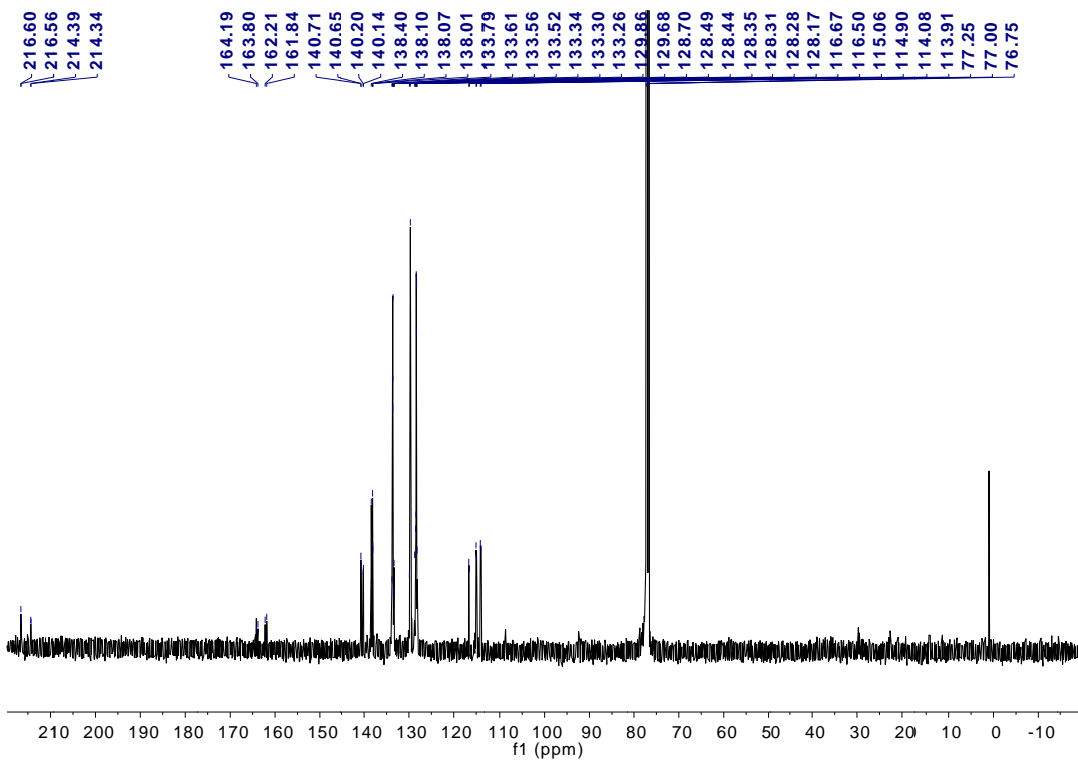


Figure S11. <sup>13</sup>C NMR (126 MHz, CDCl<sub>3</sub>, 25 °C) spectrum of **2-anti**. Assignments:  $\delta$  = 216.6, 214.4 (2d,  $^2J_{P-C}$  = 6.8 Hz, PFe(CO)<sub>2</sub>), 113.9-164.2 (m, C<sub>6</sub>H<sub>5</sub> + C<sub>6</sub>H<sub>4</sub>) ppm.

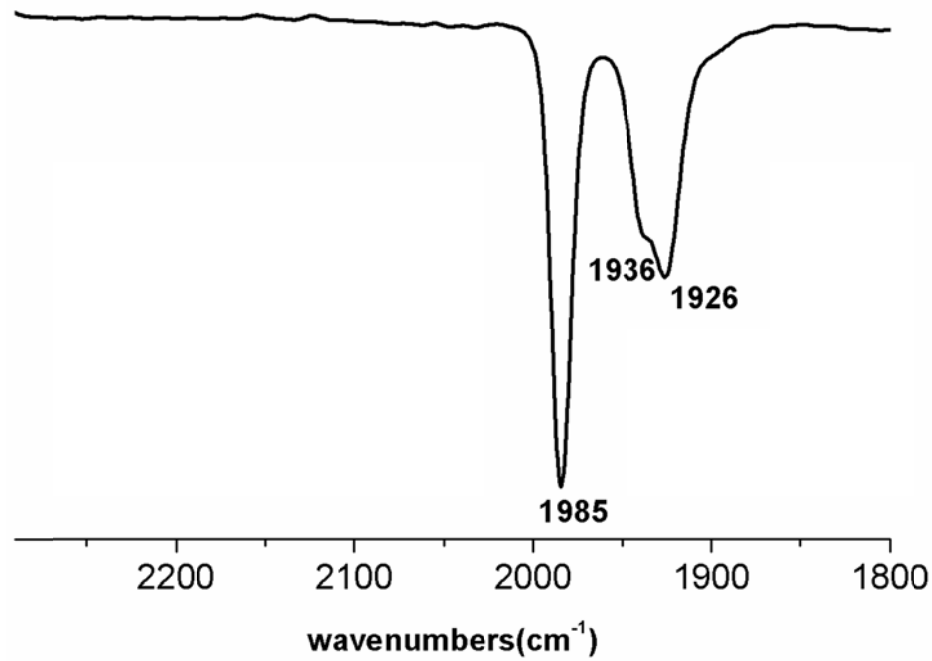


Figure S12. FT-IR (in CH<sub>2</sub>Cl<sub>2</sub>, 25 °C) spectrum of **2-syn**. Assignments:  $\nu_{CO}$  = 1985, 1936, 1926 cm<sup>-1</sup>.

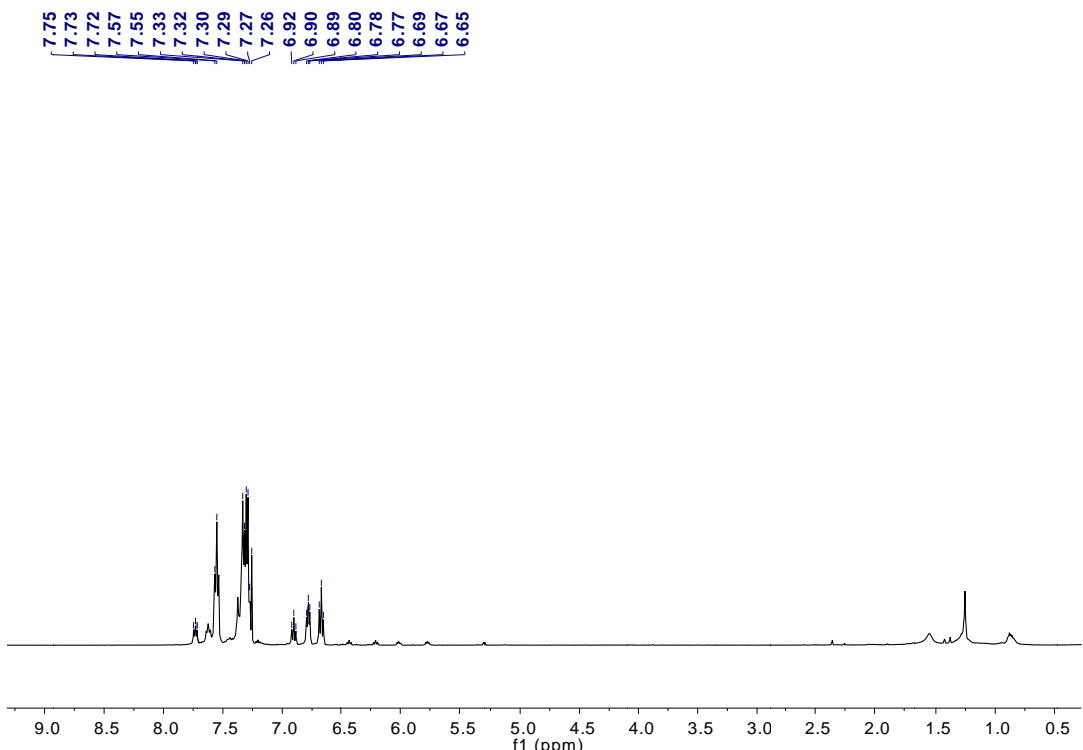


Figure S13.  $^1\text{H}$  NMR (500 MHz,  $\text{CDCl}_3$ , 25 °C) spectrum of **2-syn** in  $\text{CDCl}_3$ .  
Assignments:  $\delta = 7.75\text{-}6.65$  (m, 38H,  $6\text{C}_6\text{H}_5 + 2\text{C}_6\text{H}_4$ ) ppm.

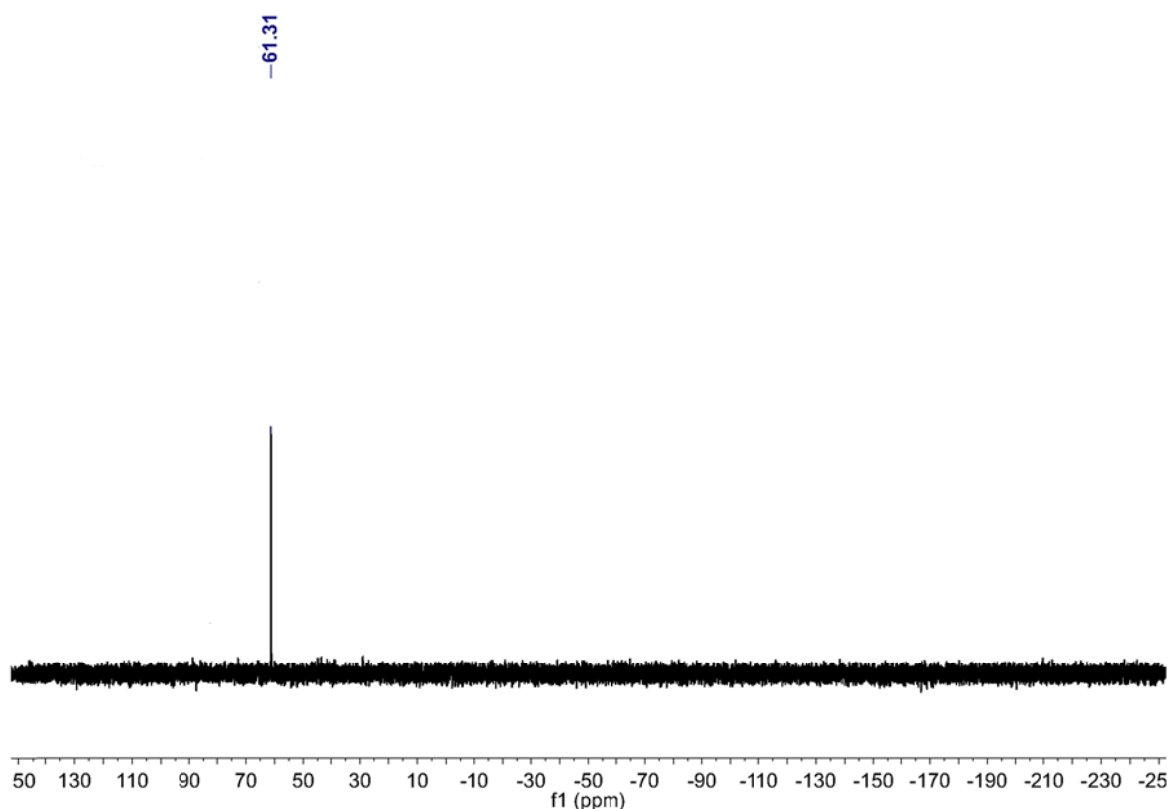


Figure S14.  $^{31}\text{P}$  NMR (202 MHz,  $\text{CDCl}_3$ , 25 °C) spectrum of **2-syn**. Assignments:  $\delta = 61.31$  ppm.

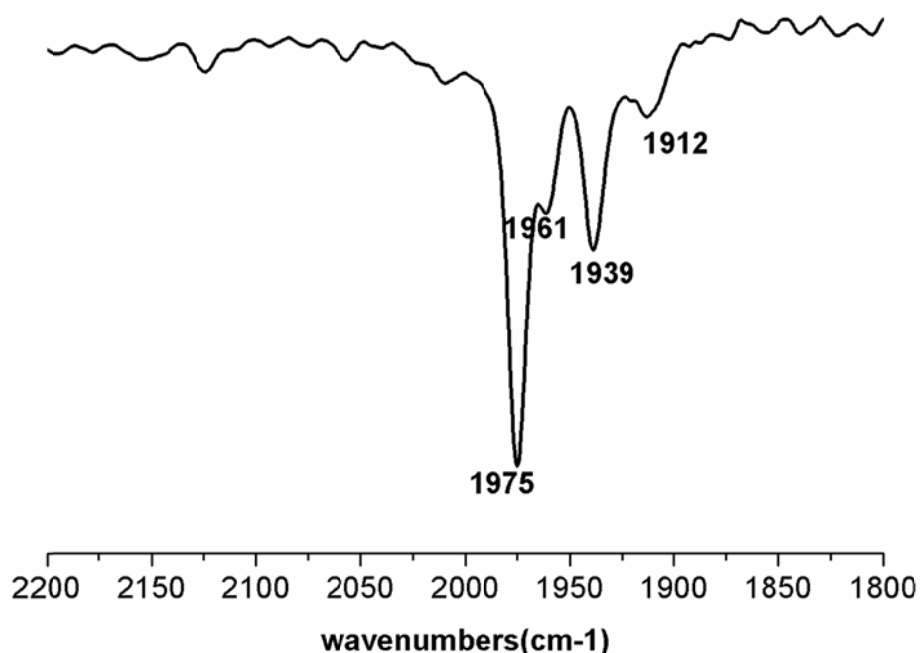


Figure S15. FT-IR (in  $\text{CH}_2\text{Cl}_2$ ,  $25^\circ\text{C}$ ) spectrum of **3** ppm.  
Assignments:  $\nu_{\text{CO}} = 1975, 1961, 1939, 1912 \text{ cm}^{-1}$ .

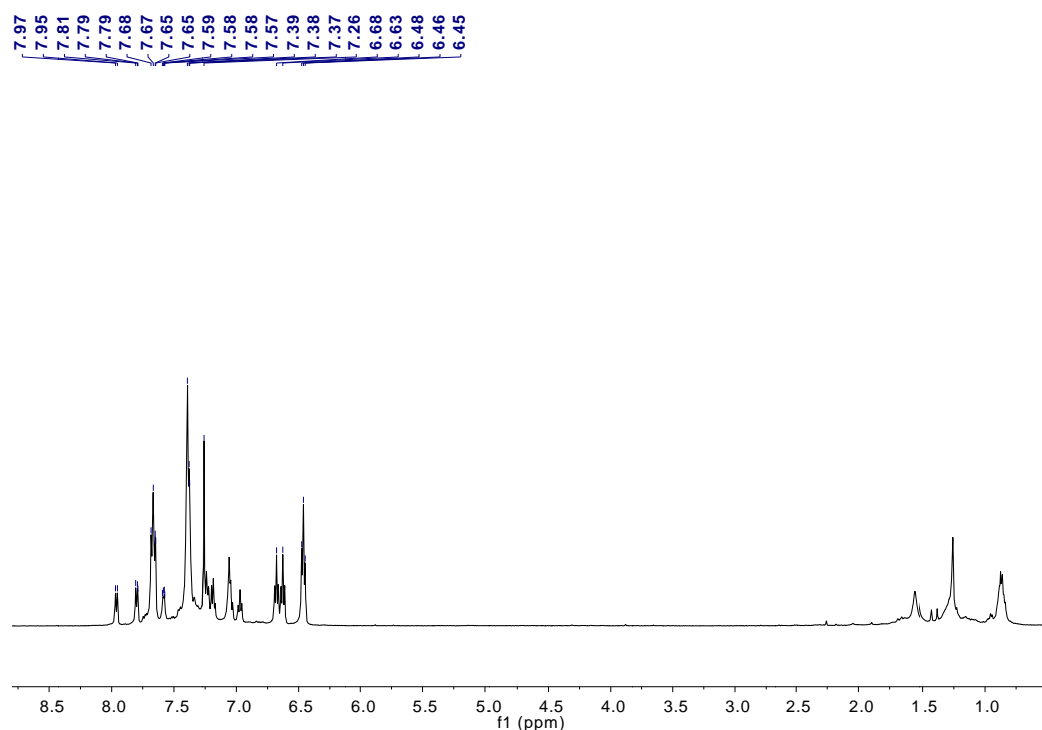


Figure S16.  $^1\text{H}$  NMR (500 MHz,  $\text{CDCl}_3$ ,  $25^\circ\text{C}$ ) spectrum of **3**. Assignments:  $\delta = 7.97\text{-}6.45$  (m, 40H, 8C<sub>6</sub>H<sub>5</sub>) ppm.

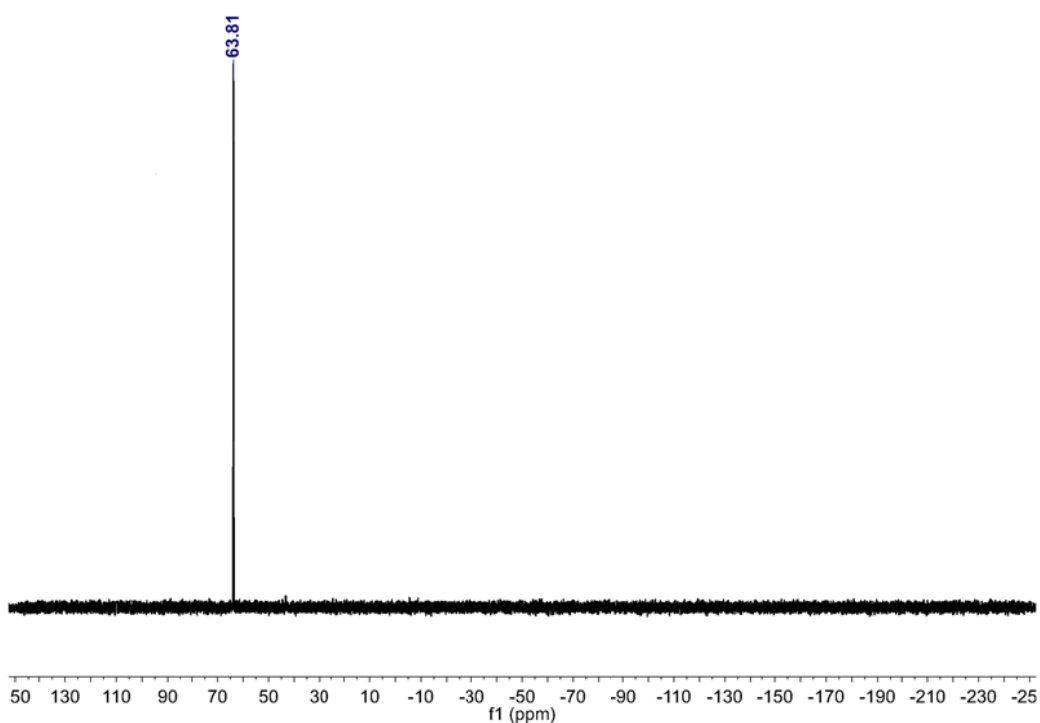


Figure S17.  $^{31}\text{P}$  NMR (202 MHz,  $\text{CDCl}_3$ , 25 °C) spectrum of **3**. *Assignments:*  $\delta = 63.81$  ppm.

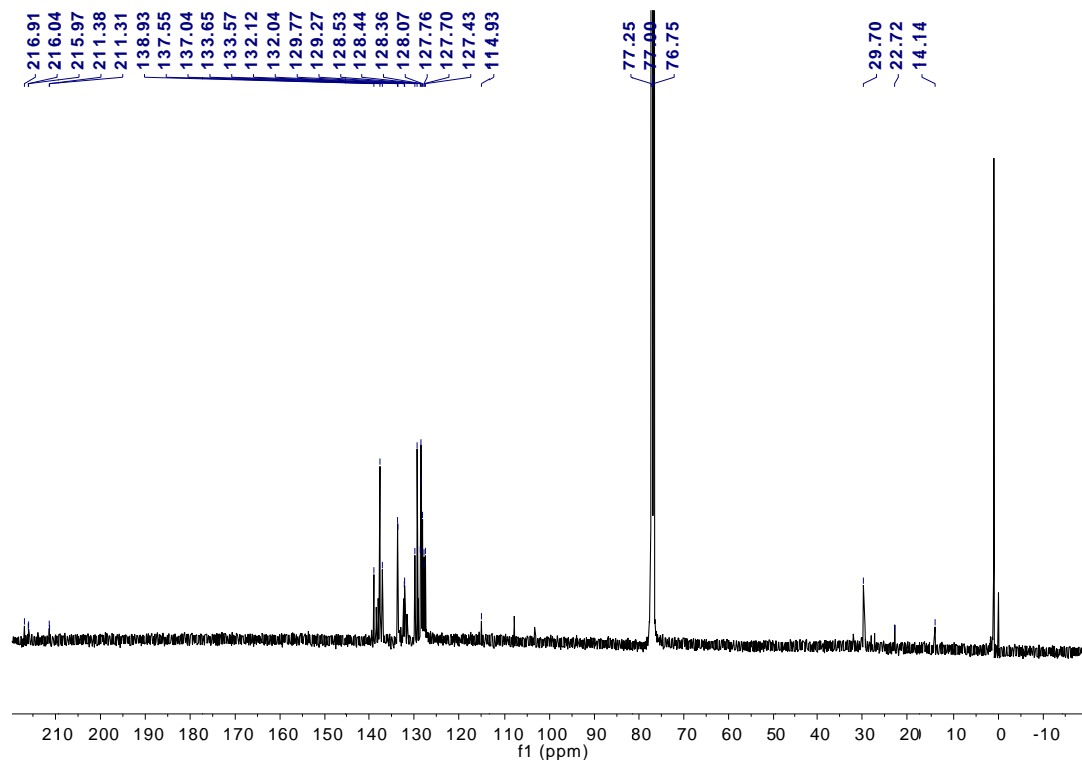


Figure S18.  $^{13}\text{C}$  NMR (126 MHz,  $\text{CDCl}_3$ , 25 °C) spectrum of **3**. *Assignments:*  $\delta = 216.9, 216.0$  (2d,  $^2J_{\text{P-C}} = 7.6$  Hz, PFe(CO)<sub>2</sub>), 115.7-139.4 (m, C<sub>6</sub>H<sub>5</sub>) ppm.

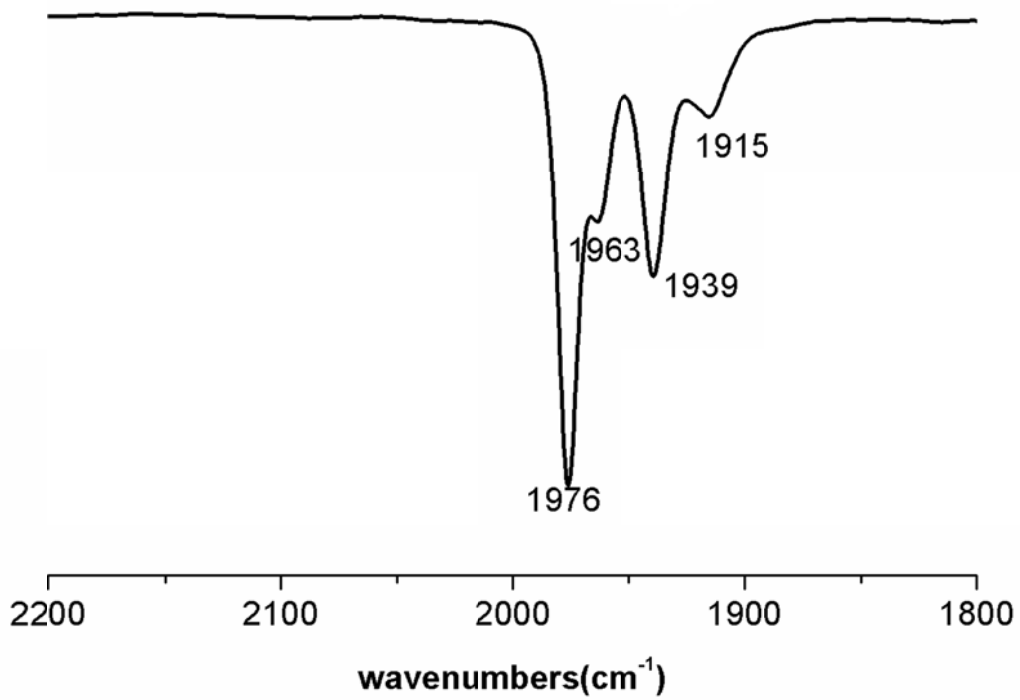


Figure S19. FT-IR (in  $\text{CH}_2\text{Cl}_2$ ,  $25^\circ\text{C}$ ) spectrum of **4**. *Assignments:*  $\nu_{\text{CO}} = 1976$ ,  $1963$ ,  $1939$ ,  $1915 \text{ cm}^{-1}$ .

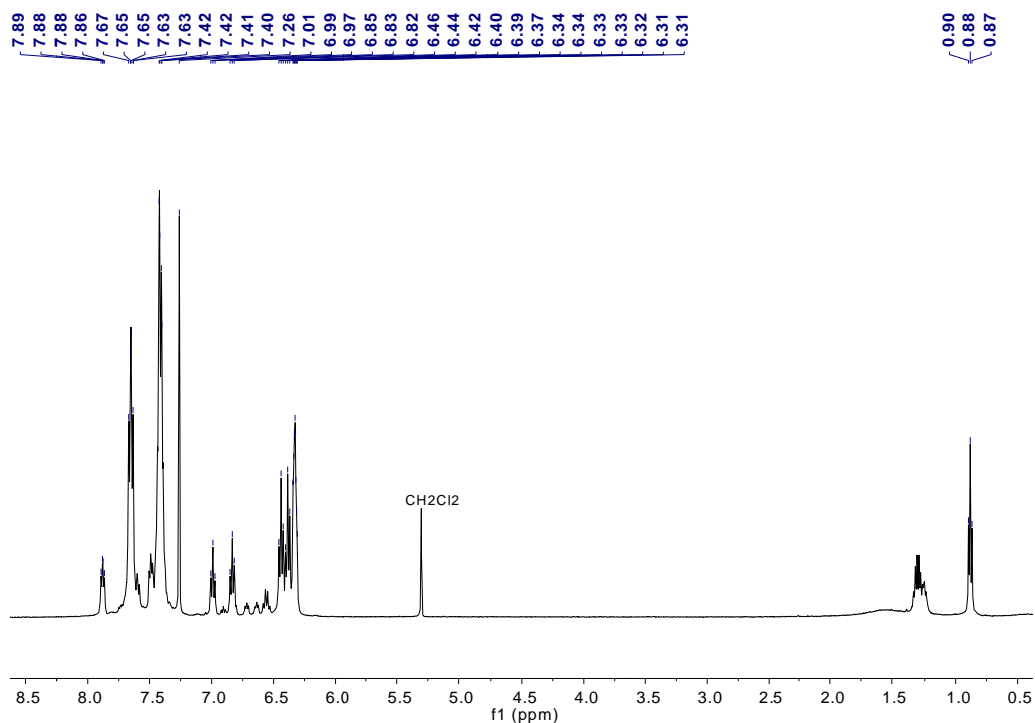


Figure S20.  $^1\text{H}$  NMR (500 MHz,  $\text{CDCl}_3$ ,  $25^\circ\text{C}$ ) spectrum of **4**. *Assignments:*  $\delta = 7.89\text{-}6.31$  (m, 38H,  $6\text{C}_6\text{H}_5 + 6\text{C}_6\text{H}_4$ ) ppm.

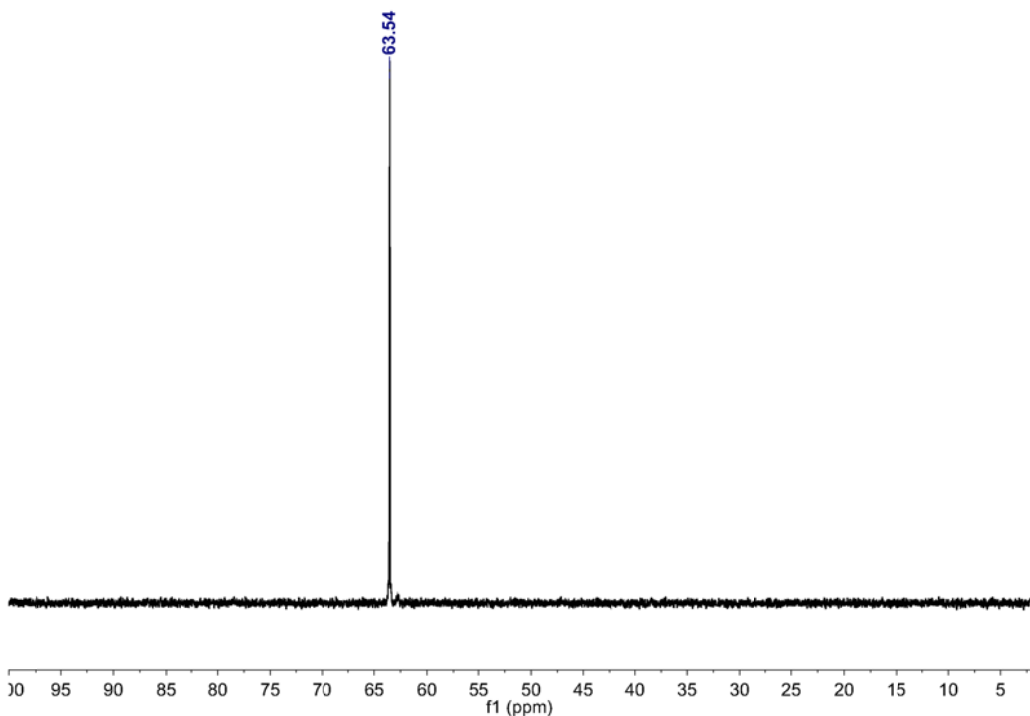


Figure S21.  $^{31}\text{P}$  NMR (202 MHz,  $\text{CDCl}_3$ , 25 °C) spectrum of **4**. *Assignments:*  $\delta = 63.54$  ppm.

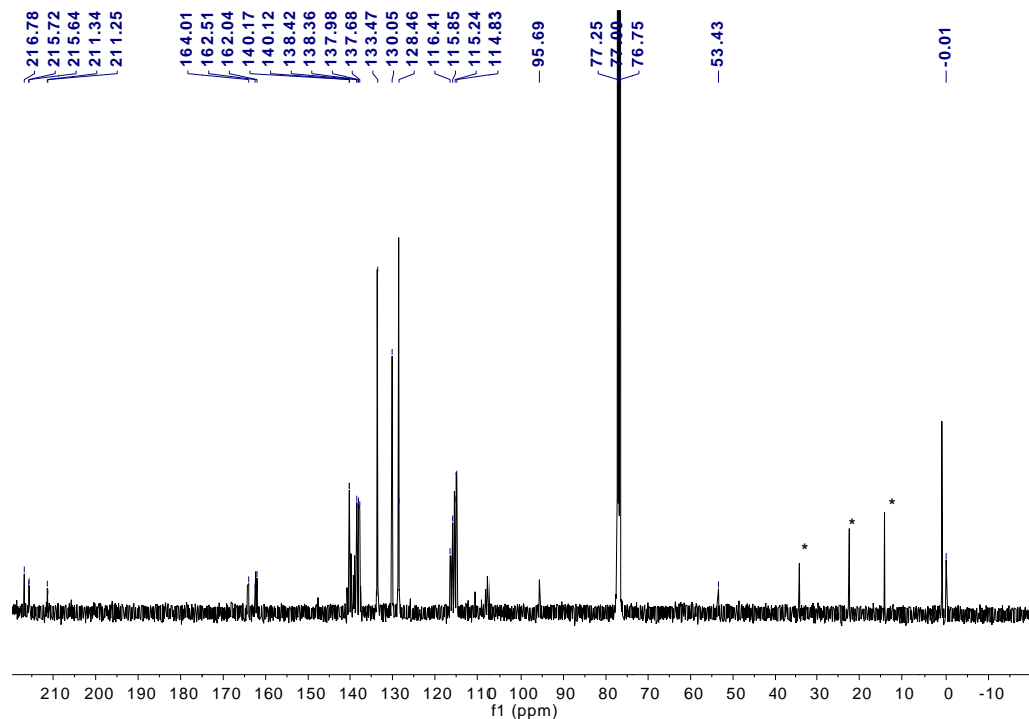


Figure S22.  $^{13}\text{C}$  NMR (126 MHz,  $\text{CDCl}_3$ , 25 °C) spectrum of **4** (\* Traces of hexane). *Assignments:*  $\delta = 216.8$  (s, FeCO), 215.6, 211.3(2d,  $^2J_{\text{P-C}} = 10.1$  Hz, PFe(CO)<sub>2</sub>) ppm, 114.8-164.0 (m, C<sub>6</sub>H<sub>5</sub> + C<sub>6</sub>H<sub>4</sub>).

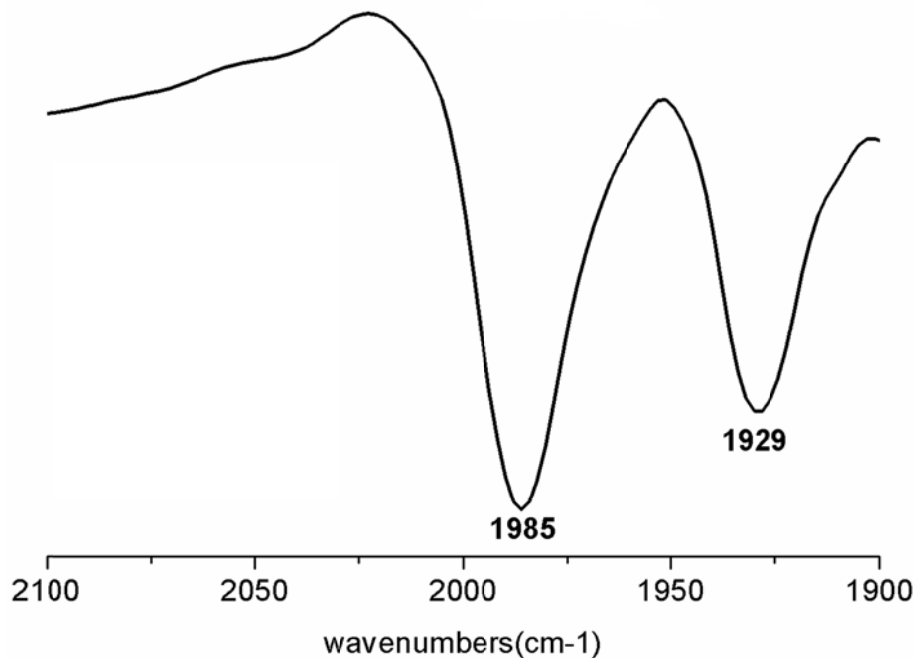


Figure S23. FT-IR (in CH<sub>2</sub>Cl<sub>2</sub>, 25°C) spectrum of **5**. Assignments:  $\nu_{CO} = 1985, 1929$  cm<sup>-1</sup>.

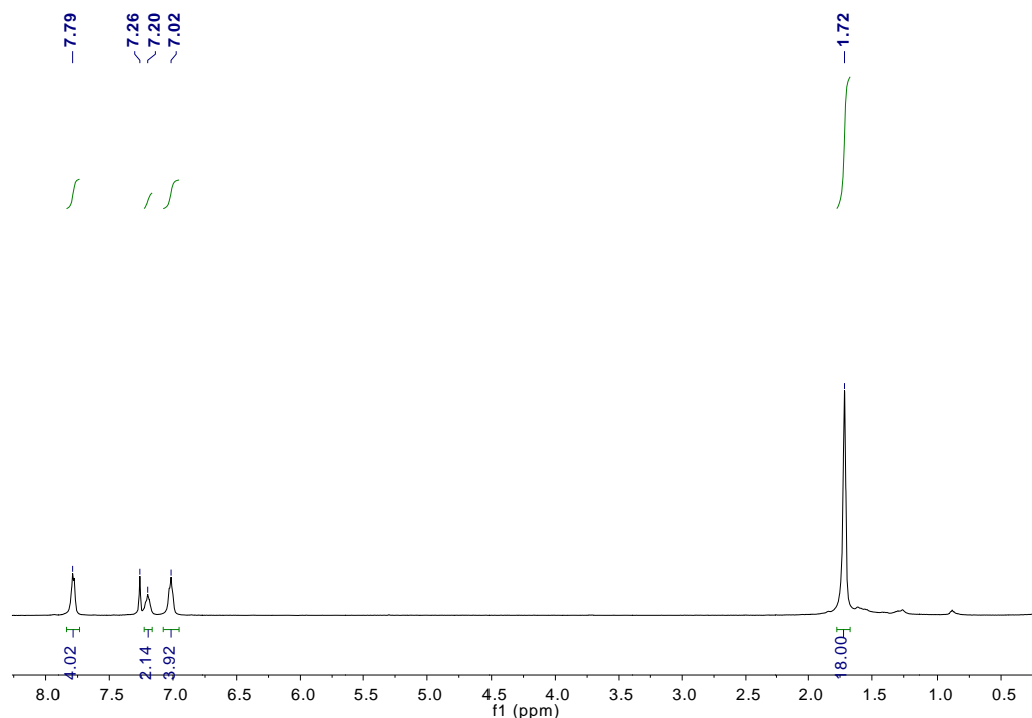


Figure S24. <sup>1</sup>H NMR (500 MHz, CDCl<sub>3</sub>, 25 °C) spectrum of **5**. Assignments:  $\delta = 7.79, 7.20, 7.02$  (3s, 10H, 2C<sub>6</sub>H<sub>5</sub>), 1.72 (s, 18H, 6CH<sub>3</sub>) ppm.

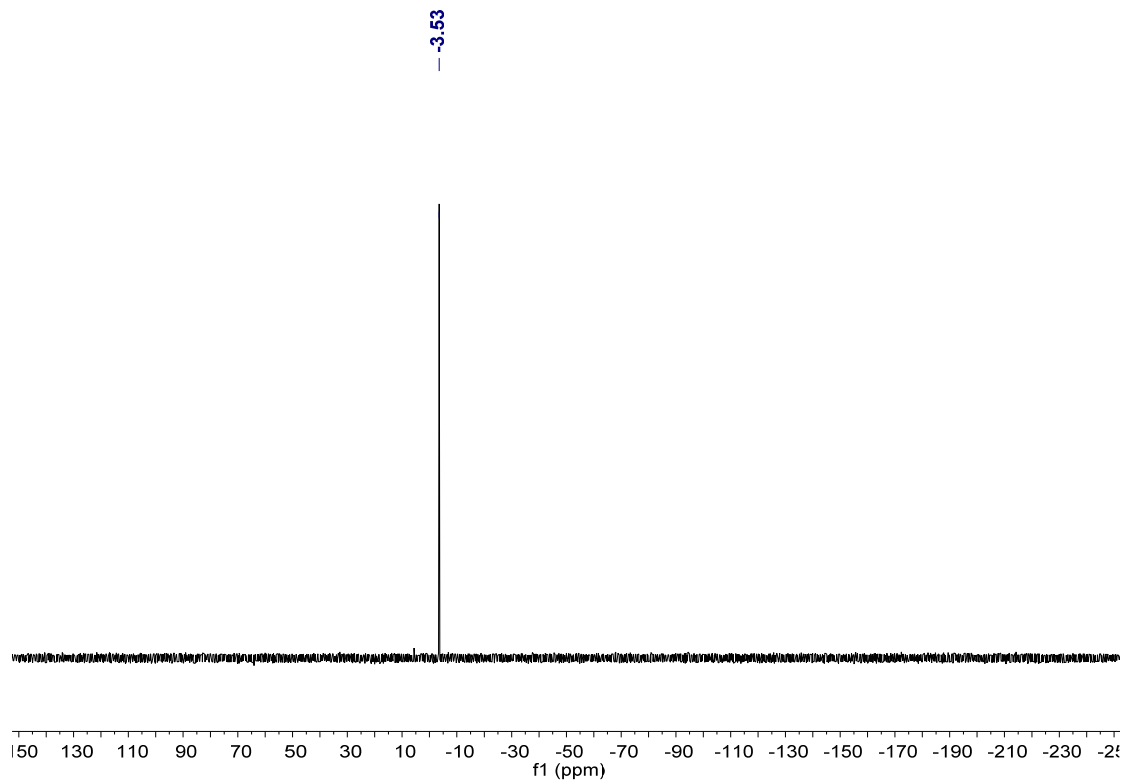


Figure S25.  $^{31}\text{P}$  NMR (202 MHz,  $\text{CDCl}_3$ , 25 °C) spectrum of **5**. *Assignments:*  $\delta = -3.53$  ppm.

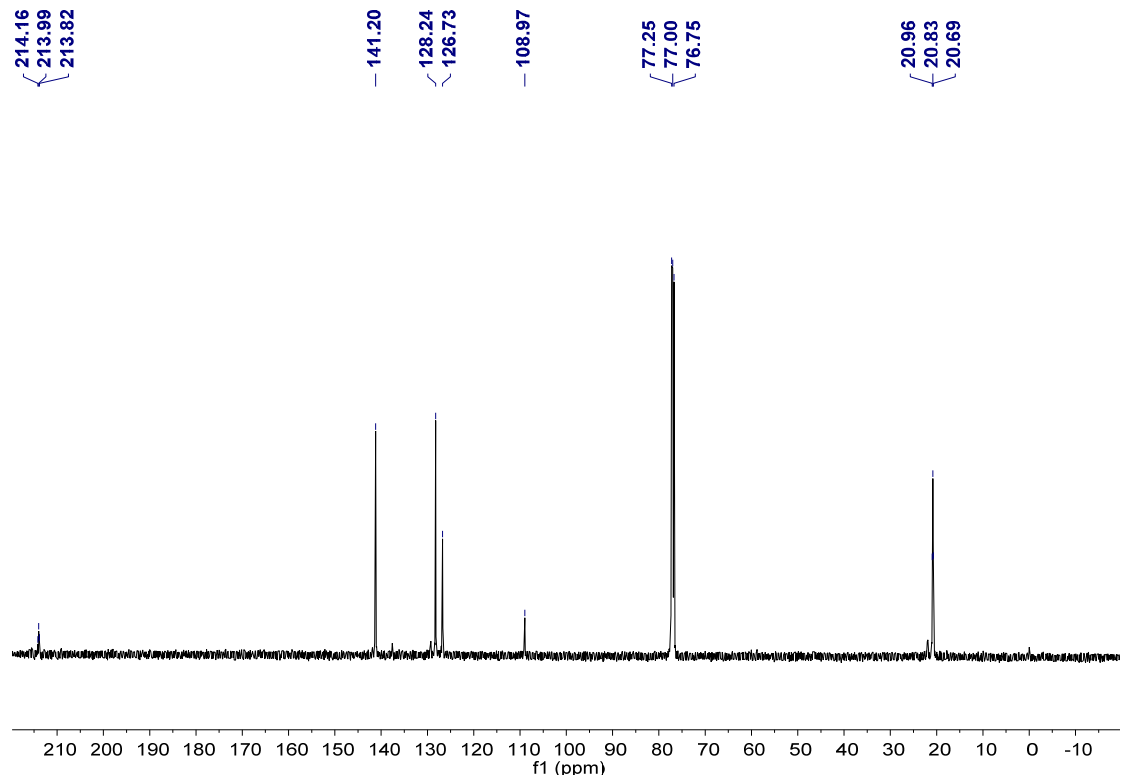


Figure S26.  $^{13}\text{C}$  NMR (126 MHz,  $\text{CDCl}_3$ , 25 °C) spectrum of **5**. *Assignments:*  $\delta = 214.0$  ( $t, J = 21.4$ ,  $\text{Fe}(\text{CO})_2$ ), 141.2, 128.2, 126.7, 109.0 ( $\text{C}_6\text{H}_5$ ), 20.8 ( $t, J_{\text{P-C}} = 17.6\text{Hz}$ ,  $\text{PCH}_3$ ) ppm.

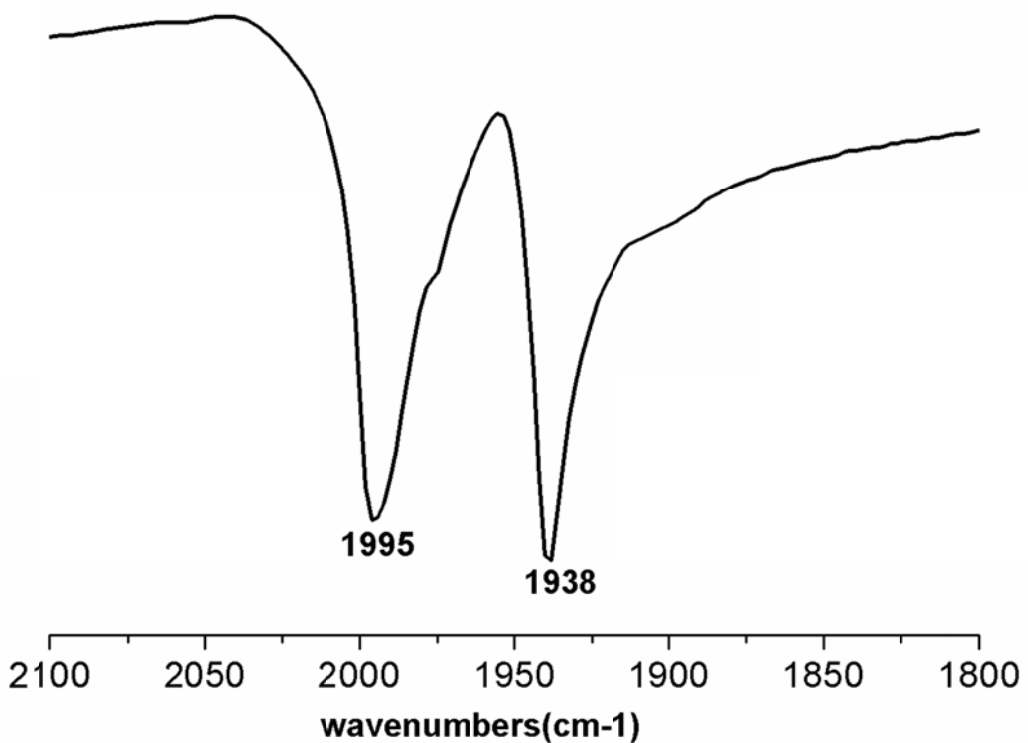


Figure S27. FT-IR (in CH<sub>2</sub>Cl<sub>2</sub>, 25°C) spectrum of **6**. *Assignments:*  $\nu_{CO} = 1995, 1938$  cm<sup>-1</sup>.

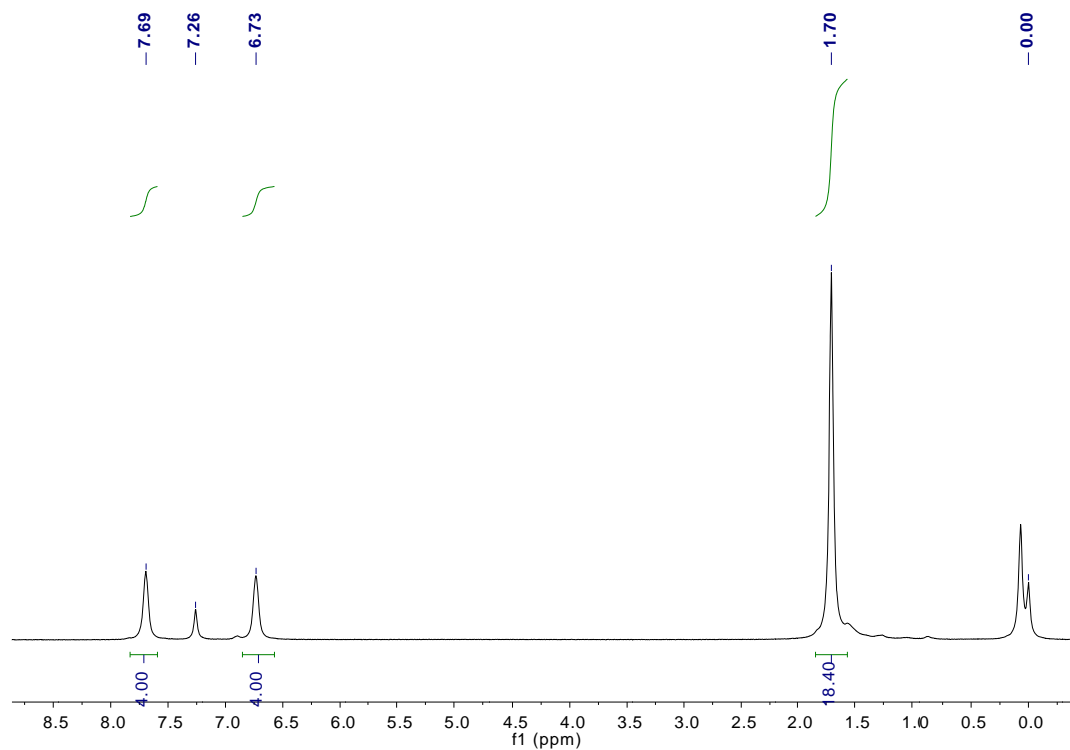


Figure S28. <sup>1</sup>H NMR (500 MHz, CDCl<sub>3</sub>, 25 °C) spectrum of **6**. *Assignments:*  $\delta = 7.69, 6.73$  (2s, 8H, 2C<sub>6</sub>H<sub>4</sub>), 1.70 (s, 18H, 6CH<sub>3</sub>) ppm.

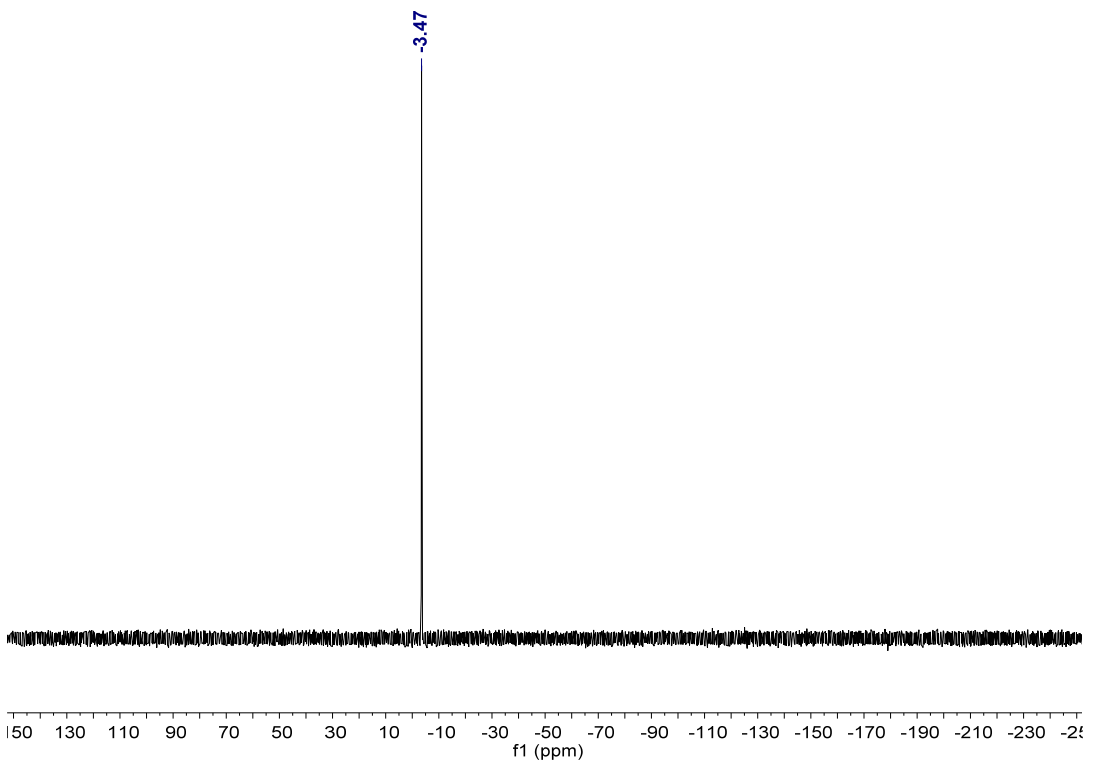


Figure S29.  $^{31}\text{P}$  NMR (202 MHz,  $\text{CDCl}_3$ , 25 °C) spectrum of **6**. *Assignments:*  $\delta =$  -3.47 ppm.

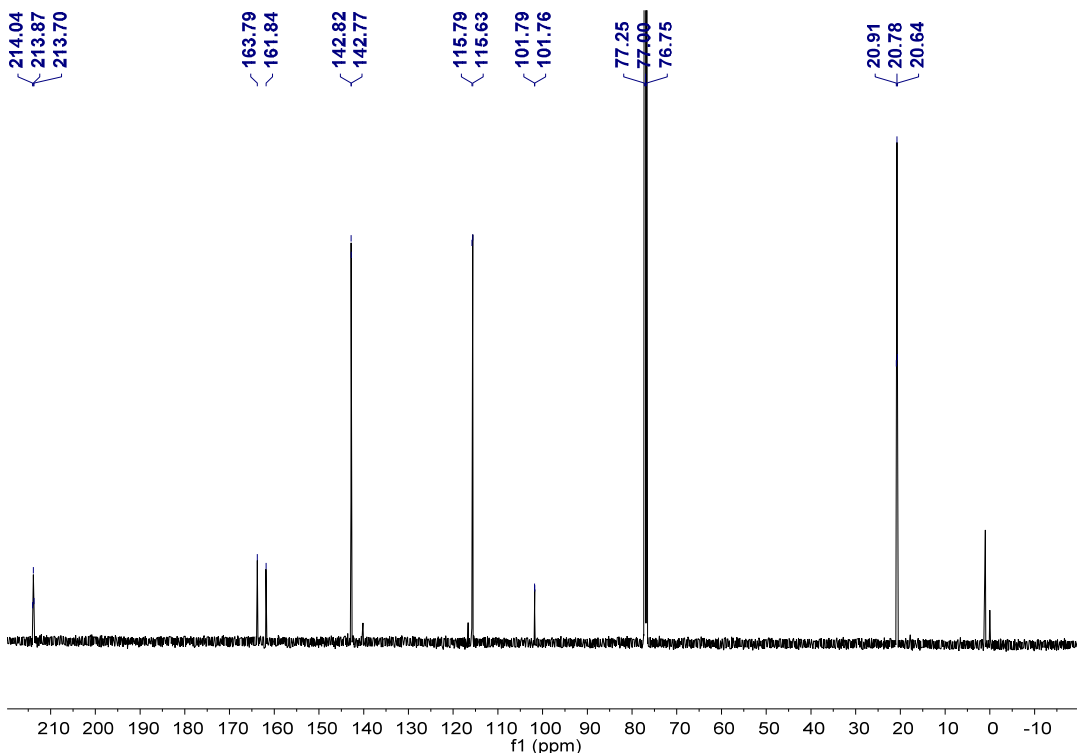


Figure S30.  $^{13}\text{C}$  NMR (126 MHz,  $\text{CDCl}_3$ , 25 °C) spectrum of **6**. *Assignments:*  $\delta =$  213.9 (t,  $J = 21.4$ ,  $\text{Fe}(\text{CO})_2$ ), 162.8 (d,  $^1J_{\text{F-C}} = 246$  Hz, *p*-C of  $\text{C}_6\text{H}_4\text{Te}$ ), 142.8 (d,  $^3J_{\text{F-C}} = 6.3$  Hz, *o*-C of  $\text{C}_6\text{H}_4\text{Te}$ ), 115.7 (d,  $^2J_{\text{F-C}} = 20.2$  Hz, *m*-C of  $\text{C}_6\text{H}_4\text{Te}$ ), 101.8 (d,  $^4J_{\text{F-C}} =$

3.8 Hz, *ipso*-C of C<sub>6</sub>H<sub>4</sub>Te), 20.8 (t,  $J_{\text{P-C}} = 17.6$ Hz, PCH<sub>3</sub>) ppm.

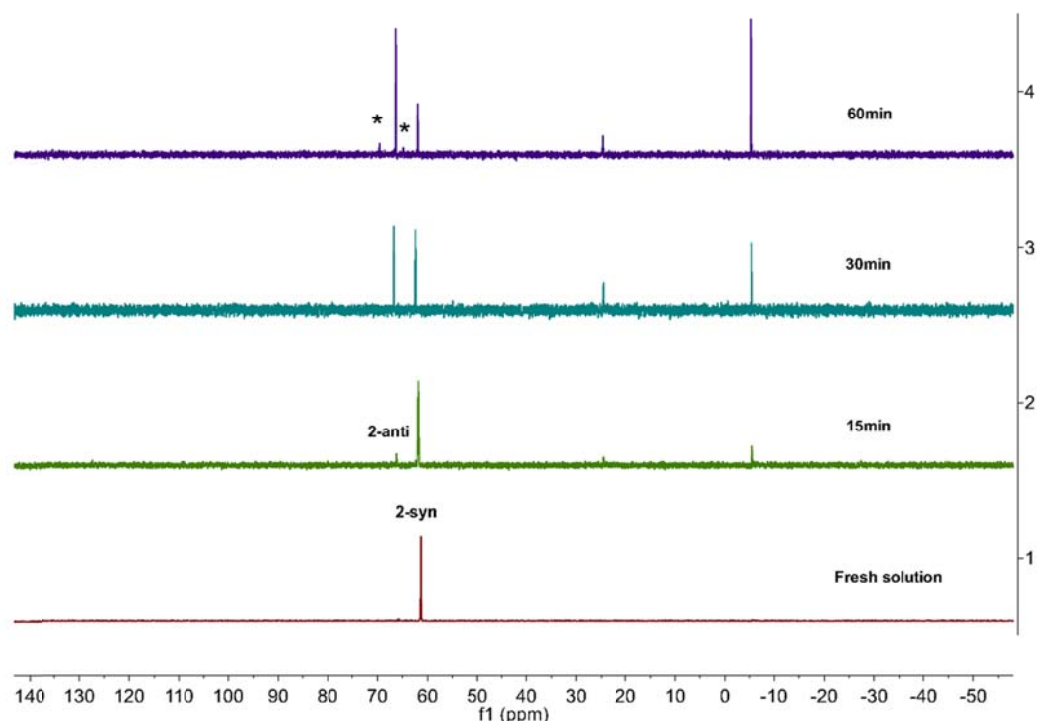


Figure S31. Slide of <sup>31</sup>P NMR of **2-syn** in toluene (100 °C).  
(\* *anti*/syn-Fe<sub>2</sub>(μ-TeC<sub>6</sub>H<sub>4</sub>-F-4)<sub>2</sub>(CO)<sub>5</sub>(Ph<sub>3</sub>P)).

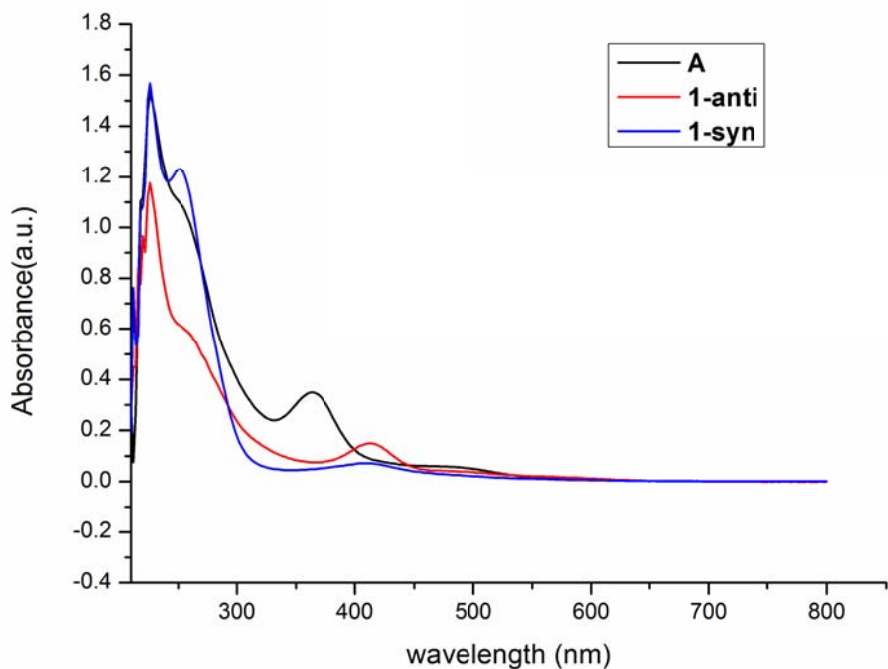


Figure S32 UV-visible spectra of **A** (black), **1-anti** (red) and **1-syn** (blue) recorded in  $\text{CH}_2\text{Cl}_2$  at 25 °C.

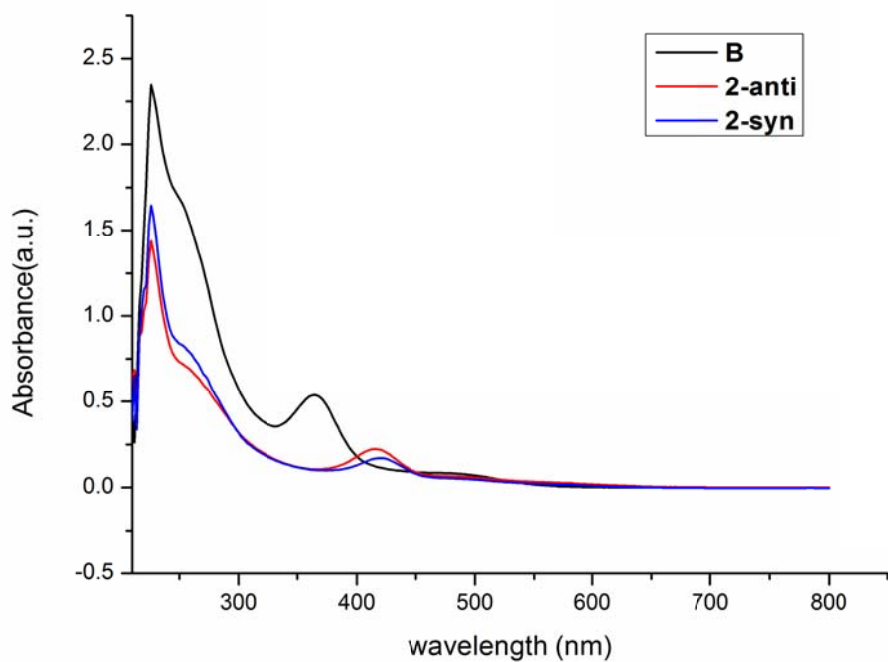


Figure S33 UV-visible spectra of **B** (black), **2-anti** (red) and **2-syn** (blue) recorded in  $\text{CH}_2\text{Cl}_2$  at 25 °C.

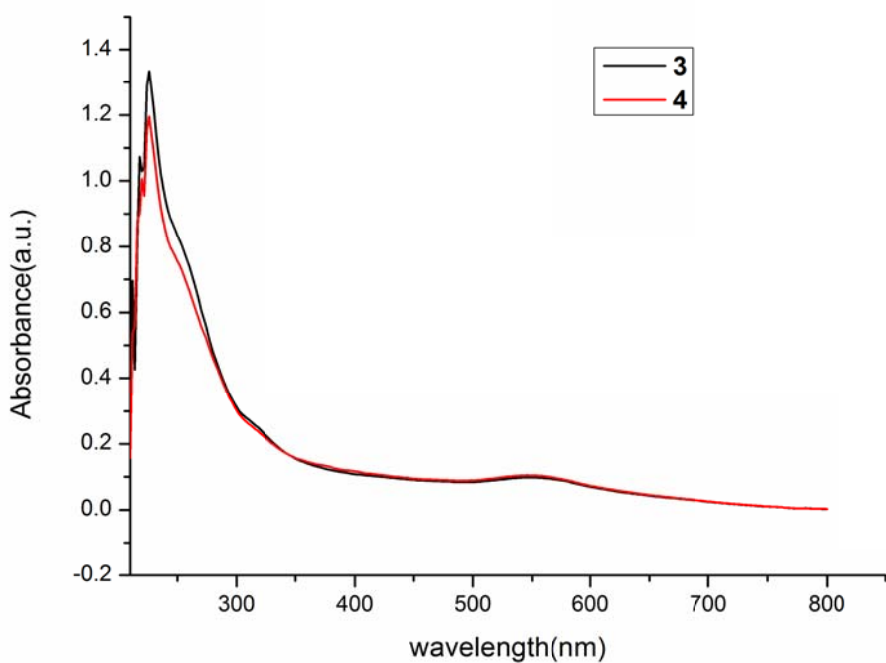


Figure S34 UV-visible spectra of **3** (black) and **4** (red) recorded in  $\text{CH}_2\text{Cl}_2$  at 25 °C.

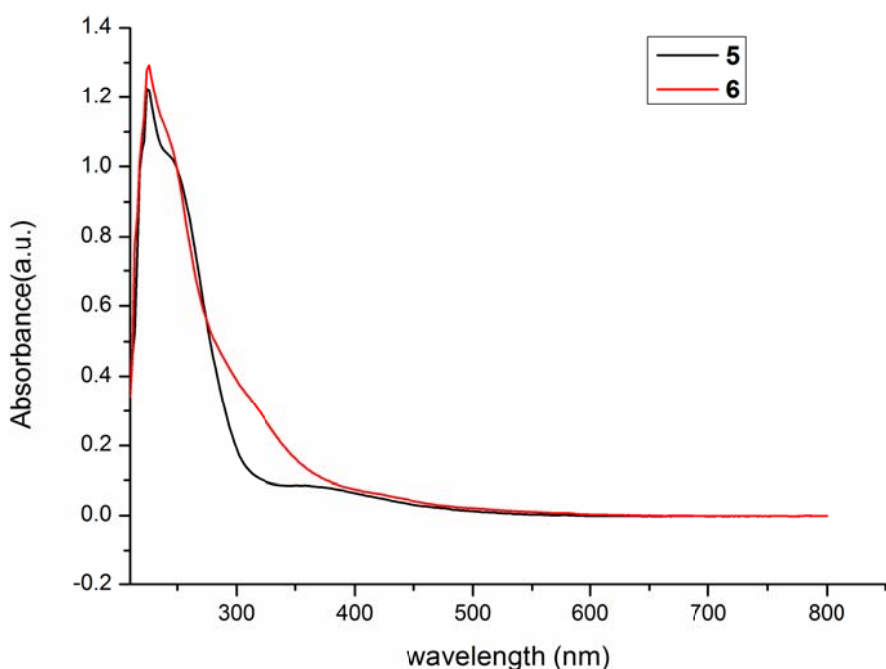


Figure S35 UV-visible spectra of **5** (black) and **6** (red) recorded in  $\text{CH}_2\text{Cl}_2$  at 25 °C.

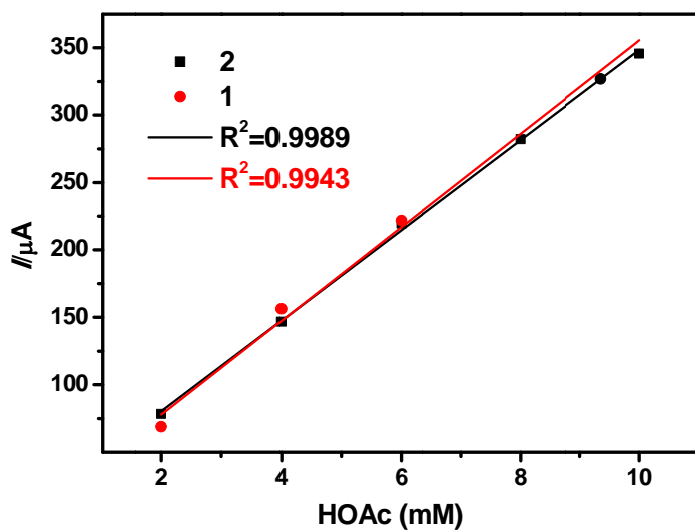


Figure S36 Dependence of current heights of the reduction events for **1** and **2** on the concentration of HOAc in  $\text{CH}_3\text{CN}$

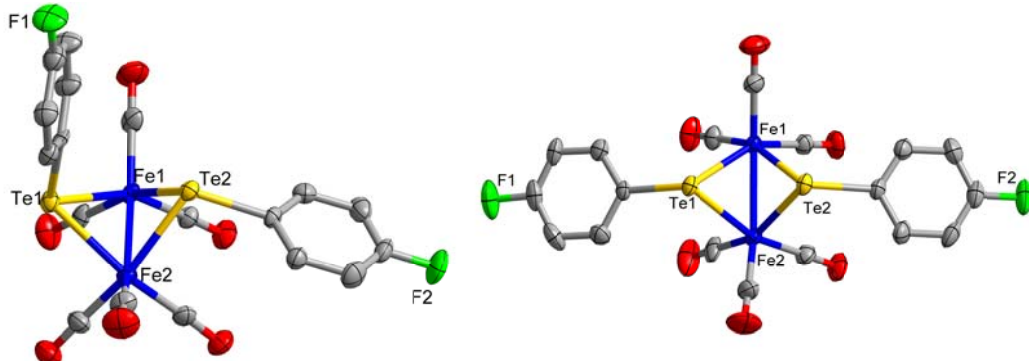


Figure S37. Molecular structures of compounds **B-anti**: (left) and **B-syn** (right) with thermal ellipsoids at 30% probability. Selected distance ( $\text{\AA}$ ) and angles ( $^\circ$ ) for **B-anti**:  
 Fe(1)-Fe(2) 2.6268(17) Te(1)-Fe(1) 2.5443(14) Te(1)-Fe(2) 2.5466(14)  
 Fe(1)-Te(1)-Fe(2) 62.13(4) Fe(2)-Te(2)-Fe(1) 61.87(4).  
 For **B-syn**: Fe(1)-Fe(2) 2.5897(12) Te(1)-Fe(1) 2.5542(9) Te(1)-Fe(2) 2.5554(9)  
 Fe(1)-Te(1)-Fe(2) 60.91(3) Fe(1)-Te(2)-Fe(2) 60.98(3)

Table S1. Crystal data and structure refinement parameters for **1-anti**, **2-anti**, **2-syn** and **4-6**.

compound	<b>1-anti</b>	<b>2-anti</b>	<b>2-syn</b>	<b>4·CH<sub>2</sub>Cl<sub>2</sub></b>	<b>5</b>	<b>6</b>
Mol formula	C <sub>52</sub> H <sub>40</sub> Fe <sub>2</sub> O <sub>4</sub> P <sub>2</sub> Te <sub>2</sub>	C <sub>52</sub> H <sub>38</sub> F <sub>2</sub> Fe <sub>2</sub> O <sub>4</sub> P <sub>2</sub> Te <sub>2</sub>	C <sub>52</sub> H <sub>38</sub> F <sub>2</sub> Fe <sub>2</sub> O <sub>4</sub> P <sub>2</sub> Te <sub>2</sub>	C <sub>79</sub> H <sub>56</sub> Cl <sub>2</sub> F <sub>6</sub> Fe <sub>4</sub> O <sub>6</sub> P <sub>2</sub> Te <sub>6</sub>	C <sub>20</sub> H <sub>28</sub> FeO <sub>2</sub> P <sub>2</sub> Te <sub>2</sub>	C <sub>20</sub> H <sub>26</sub> F <sub>2</sub> FeO <sub>2</sub> P <sub>2</sub> Te <sub>2</sub>
Mol wt	1157.68	1193.66	1193.66	2337.08	673.41	709.40
Wavelength (Å)	0.71073	1.54178	0.71073	0.71073	0.71073	0.71073
Cryst syst	Trigonal	Monoclinic	Monoclinic	Monoclinic	Monoclinic	Triclinic
Space group	P3(1)	P2(1)	P2(1)/n	P2(1)/c	P2(1)/c	P-1
<i>a</i> /Å	11.0760(11)	14.4916(10)	15.7523(13)	10.5984(9)	16.7672(15)	10.5443(8)
<i>b</i> /Å	11.0760(11)	21.8071(11)	18.9568(16)	28.117(3)	16.7707(15)	11.4210(9)
<i>c</i> /Å	34.329(3)	17.8631(12)	17.0727(14)	27.262(3)	9.2532(8)	12.3027(11)
$\alpha$ /deg	90	90	90	90	90	73.951(2)
$\beta$ /deg	90	112.899(4)	108.237(3)	100.664(3)	104.480(4)	76.513(2)
$\gamma$ /deg	120	90	90	90	90	66.4360(10)
<i>V</i> /Å <sup>3</sup>	3647.2(6)	5200.2(6)	4842.1(7)	7983.7(13)	2171.1(10)	1292.38(18)
<i>Z</i>	3	4	4	4	4	2
<i>D</i> <sub>v</sub> /gcm <sup>-3</sup>	1.581	1.525	1.637	1.944	1.775	1.823
abs coeff/mm <sup>-1</sup>	1.881	14.128	1.898	3.033	3.008	2.947
F(000)	1710	2344	2344	4448	1296	680
index ranges	-13 ≤ <i>h</i> ≤ 13 -13 ≤ <i>k</i> ≤ 13 -40 ≤ <i>l</i> ≤ 34	-17 ≤ <i>h</i> ≤ 14 -25 ≤ <i>k</i> ≤ 22 -21 ≤ <i>l</i> ≤ 21	-18 ≤ <i>h</i> ≤ 18 -22 ≤ <i>k</i> ≤ 17 -20 ≤ <i>l</i> ≤ 19	-12 ≤ <i>h</i> ≤ 11 -33 ≤ <i>k</i> ≤ 27 -31 ≤ <i>l</i> ≤ 32	-19 ≤ <i>h</i> ≤ 19 -16 ≤ <i>k</i> ≤ 19 -10 ≤ <i>l</i> ≤ 11	-12 ≤ <i>h</i> ≤ 12 -7 ≤ <i>k</i> ≤ 13 -13 ≤ <i>l</i> ≤ 14
no. of reflns	18484	34095	24398	14068	12345	6503
no. of indepreflns	6887	13943	8538	40681	4431	4471
Goodness of fit	1.037	1.034	1.018	1.041	1.062	1.064
R	0.0731	0.0579,	0.0565,	0.0522	0.0309	0.0391
R <sub>w</sub>	0.1625	0.1351	0.1164	0.1413	0.0741	0.0796

Table S2 Selected distances (Å) and angles (°) for **1-anti**.

<b>1-anti</b>			
Te(1)-Fe(1)	2.559(3)	Fe(1)-C(1)	1.77(2)
Te(1)-Fe(2)	2.574(3)	Fe(1)-P(1)	2.269(6)
Te(2)-C(47)	2.146(10)	Fe(1)-Fe(2)	2.653(4)
Te(2)-Fe(2)	2.580(3)	Fe(2)-C(3)	1.760(19)
Te(2)-Fe(1)	2.597(3)	Fe(2)-C(4)	1.77(3)
Fe(1)-C(2)	1.733(18)	Fe(2)-P(2)	2.253(6)
C(2)-Fe(1)-C(1)	86.1(11)	C(3)-Fe(2)-C(4)	91.5(11)
C(2)-Fe(1)-P(1)	98.7(8)	C(3)-Fe(2)-P(2)	99.0(7)
C(1)-Fe(1)-P(1)	96.5(7)	C(4)-Fe(2)-P(2)	94.9(7)
C(2)-Fe(1)-Te(1)	91.9(9)	C(3)-Fe(2)-Te(1)	92.6(7)
C(1)-Fe(1)-Te(1)	159.5(7)	C(4)-Fe(2)-Te(1)	153.8(7)
P(1)-Fe(1)-Te(1)	103.96(18)	P(2)-Fe(2)-Te(1)	109.99(17)
C(2)-Fe(1)-Te(2)	153.3(8)	C(3)-Fe(2)-Te(2)	155.3(7)

C(1)-Fe(1)-Te(2)	90.8(7)	C(4)-Fe(2)-Te(2)	83.8(7)
P(1)-Fe(1)-Te(2)	107.92(17)	P(2)-Fe(2)-Te(2)	105.53(16)
Te(1)-Fe(1)-Te(2)	81.83(9)	Te(1)-Fe(2)-Te(2)	81.90(9)
C(2)-Fe(1)-Fe(2)	95.7(8)	C(3)-Fe(2)-Fe(1)	97.1(7)
C(1)-Fe(1)-Fe(2)	100.7(7)	C(4)-Fe(2)-Fe(1)	95.3(7)
P(1)-Fe(1)-Fe(2)	158.2(2)	P(2)-Fe(2)-Fe(1)	160.74(18)
Te(1)-Fe(1)-Fe(2)	59.14(9)	Te(1)-Fe(2)-Fe(1)	58.59(9)
Te(2)-Fe(1)-Fe(2)	58.83(9)	Te(2)-Fe(2)-Fe(1)	59.49(9)

Table S3 Selected distances ( $\text{\AA}$ ) and angles ( $^\circ$ ) for **2-anti**.

<b>2-anti</b>			
Te(1)-Fe(1)	2.569(3)	Fe(1)-C(1)	1.765(18)
Te(1)-Fe(2)	2.560(3)	Fe(1)-C(2)	1.77(2)
Te(2)-Fe(2)	2.561(3)	Fe(1)-P(1)	2.244(5)
Te(2)-Fe(1)	2.582(3)	Fe(1)-Fe(2)	2.631(4)
Fe(2)-P(2)	2.224(5)	Fe(2)-C(3)	1.76(2)
Te(2)-Fe(2)	2.561(3)	Fe(2)-C(4)	1.80(2)
C(1)-Fe(1)-C(2)	95.7(9)	C(3)-Fe(2)-C(4)	94.8(9)
C(1)-Fe(1)-P(1)	94.8(5)	C(3)-Fe(2)-P(2)	95.6(6)
C(2)-Fe(1)-P(1)	92.8(7)	C(4)-Fe(2)-P(2)	95.6(8)
C(1)-Fe(1)-Te(1)	84.7(6)	C(3)-Fe(2)-Te(2)	156.3(6)
C(2)-Fe(1)-Te(1)	153.1(7)	C(4)-Fe(2)-Te(2)	90.0(6)
P(1)-Fe(1)-Te(1)	114.02(16)	P(2)-Fe(2)-Te(2)	107.00(15)
C(1)-Fe(1)-Te(2)	156.3(5)	C(3)-Fe(2)-Te(1)	84.9(6)
C(2)-Fe(1)-Te(2)	89.3(6)	C(4)-Fe(2)-Te(1)	153.0(8)
P(1)-Fe(1)-Te(2)	108.14(15)	P(2)-Fe(2)-Te(1)	111.37(18)
Te(1)-Fe(1)-Te(2)	80.58(8)	Te(2)-Fe(2)-Te(1)	80.44(8)
C(1)-Fe(1)-Fe(2)	97.4(5)	C(3)-Fe(2)-Fe(1)	97.4(6)
C(2)-Fe(1)-Fe(2)	94.1(7)	C(4)-Fe(2)-Fe(1)	94.3(7)
P(1)-Fe(1)-Fe(2)	165.40(18)	P(2)-Fe(2)-Fe(1)	162.95(18)
Te(1)-Fe(1)-Fe(2)	59.38(8)	Te(2)-Fe(2)-Fe(1)	59.07(8)
Te(2)-Fe(1)-Fe(2)	59.11(8)	Te(1)-Fe(2)-Fe(1)	59.13(8)

Table S4 Selected distances ( $\text{\AA}$ ) and angles ( $^\circ$ ) for **2-syn**.

<b>2-syn</b>			
Te(1)-Fe(1)	2.5759(9)	Fe(1)-C(2)	1.759(8)
Te(1)-Fe(2)	2.5856(10)	Fe(1)-C(1)	1.768(7)
Te(2)-C(11)	2.144(6)	Fe(1)-P(1)	2.2818(18)
Te(2)-Fe(1)	2.5882(9)	Fe(1)-Fe(2)	2.6516(12)
Te(2)-Fe(2)	2.5957(9)	Fe(2)-C(4)	1.749(7)
F(1)-C(14)	1.379(8)	Fe(2)-C(3)	1.764(8)
F(2)-C(8)	1.373(7)	Fe(2)-P(2)	2.2735(18)
C(2)-Fe(1)-C(1)	88.7(3)	C(4)-Fe(2)-C(3)	88.8(3)
C(2)-Fe(1)-P(1)	100.3(2)	C(4)-Fe(2)-P(2)	101.3(2)

C(1)-Fe(1)-P(1)	101.9(2)	C(3)-Fe(2)-P(2)	100.2(2)
C(2)-Fe(1)-Te(1)	90.5(2)	C(4)-Fe(2)-Te(1)	93.5(2)
C(1)-Fe(1)-Te(1)	154.0(2)	C(3)-Fe(2)-Te(1)	157.0(2)
P(1)-Fe(1)-Te(1)	103.80(5)	P(2)-Fe(2)-Te(1)	101.68(5)
C(2)-Fe(1)-Te(2)	157.3(2)	C(4)-Fe(2)-Te(2)	154.4(2)
C(1)-Fe(1)-Te(2)	90.9(2)	C(3)-Fe(2)-Te(2)	88.4(2)
P(1)-Fe(1)-Te(2)	102.06(5)	P(2)-Fe(2)-Te(2)	104.19(5)
Te(1)-Fe(1)-Te(2)	80.00(3)	Te(1)-Fe(2)-Te(2)	79.68(3)
C(2)-Fe(1)-Fe(2)	98.0(2)	C(4)-Fe(2)-Fe(1)	96.2(2)
C(1)-Fe(1)-Fe(2)	95.1(2)	C(3)-Fe(2)-Fe(1)	98.1(2)
P(1)-Fe(1)-Fe(2)	155.20(6)	P(2)-Fe(2)-Fe(1)	154.75(6)
Te(1)-Fe(1)-Fe(2)	59.27(3)	Te(1)-Fe(2)-Fe(1)	58.91(3)
Te(2)-Fe(1)-Fe(2)	59.37(3)	Te(2)-Fe(2)-Fe(1)	59.10(3)

Table S5 Selected distances ( $\text{\AA}$ ) and angles ( $^\circ$ ) for **4**.

<b>4</b>			
Fe(1)-C(1)	1.735(10)	Fe(3)-C(4)	1.755(10)
Fe(1)-C(2)	1.748(11)	Fe(3)-Te(3)	2.5018(14)
Fe(1)-P(1)	2.244(3)	Fe(3)-Te(4)	2.5099(14)
Fe(1)-Te(1)	2.5230(14)	Fe(3)-Te(5)	2.5417(14)
Fe(1)-Te(2)	2.5731(13)	Fe(3)-Te(6)	2.5874(14)
Fe(1)-Fe(2)	2.6731(17)	Fe(3)-Fe(4)	2.6822(18)
Fe(2)-C(3)	1.765(10)	Fe(4)-C(5)	1.747(12)
Fe(2)-Te(4)	2.5007(13)	Fe(4)-C(6)	1.760(13)
Fe(2)-Te(3)	2.5174(14)	Fe(4)-P(2)	2.253(3)
Fe(2)-Te(1)	2.5537(13)	Fe(4)-Te(5)	2.5122(15)
Fe(2)-Te(2)	2.6009(13)	Fe(4)-Te(6)	2.5667(15)
Fe(2)-Fe(3)	2.9273(17)		
C(1)-Fe(1)-C(2)	94.2(4)	C(4)-Fe(3)-Te(3)	96.1(3)
C(1)-Fe(1)-P(1)	99.4(3)	C(4)-Fe(3)-Te(4)	95.7(4)
C(2)-Fe(1)-P(1)	92.8(3)	Te(3)-Fe(3)-Te(4)	108.04(5)
C(1)-Fe(1)-Te(1)	88.9(3)	C(4)-Fe(3)-Te(5)	91.7(3)
C(2)-Fe(1)-Te(1)	161.5(3)	Te(3)-Fe(3)-Te(5)	153.27(6)
P(1)-Fe(1)-Te(1)	104.74(8)	Te(4)-Fe(3)-Te(5)	96.52(5)
C(1)-Fe(1)-Te(2)	149.0(3)	C(4)-Fe(3)-Te(6)	160.2(4)
C(2)-Fe(1)-Te(2)	86.8(3)	Te(3)-Fe(3)-Te(6)	83.74(4)
P(1)-Fe(1)-Te(2)	111.49(8)	Te(4)-Fe(3)-Te(6)	103.24(5)
Te(1)-Fe(1)-Te(2)	81.25(4)	Te(5)-Fe(3)-Te(6)	80.44(4)
C(1)-Fe(1)-Fe(2)	90.4(3)	C(4)-Fe(3)-Fe(4)	102.2(3)
C(2)-Fe(1)-Fe(2)	102.9(3)	Te(3)-Fe(3)-Fe(4)	95.90(5)
P(1)-Fe(1)-Fe(2)	160.91(9)	Te(4)-Fe(3)-Fe(4)	148.34(6)
Te(1)-Fe(1)-Fe(2)	58.79(4)	Te(5)-Fe(3)-Fe(4)	57.41(4)
Te(2)-Fe(1)-Fe(2)	59.40(4)	Te(6)-Fe(3)-Fe(4)	58.26(4)
C(3)-Fe(2)-Te(4)	97.9(3)	C(4)-Fe(3)-Fe(2)	93.0(3)

C(3)-Fe(2)-Te(3)	96.4(3)	Te(3)-Fe(3)-Fe(2)	54.57(4)
Te(4)-Fe(2)-Te(3)	107.84(5)	Te(4)-Fe(3)-Fe(2)	54.11(4)
C(3)-Fe(2)-Te(1)	90.2(3)	Te(5)-Fe(3)-Fe(2)	150.57(6)
Te(4)-Fe(2)-Te(1)	151.96(6)	Te(6)-Fe(3)-Fe(2)	102.84(5)
Te(3)-Fe(2)-Te(1)	97.76(5)	Fe(4)-Fe(3)-Fe(2)	148.39(6)
C(3)-Fe(2)-Te(2)	161.0(3)	C(5)-Fe(4)-C(6)	92.3(5)
Te(4)-Fe(2)-Te(2)	83.84(4)	C(5)-Fe(4)-P(2)	98.7(3)
Te(3)-Fe(2)-Te(2)	101.02(5)	C(6)-Fe(4)-P(2)	91.3(3)
Te(1)-Fe(2)-Te(2)	80.14(4)	C(5)-Fe(4)-Te(5)	90.2(3)
C(3)-Fe(2)-Fe(1)	102.6(3)	C(6)-Fe(4)-Te(5)	163.0(3)
Te(4)-Fe(2)-Fe(1)	94.31(5)	P(2)-Fe(4)-Te(5)	104.97(9)
Te(3)-Fe(2)-Fe(1)	148.40(6)	C(5)-Fe(4)-Te(6)	147.3(3)
Te(1)-Fe(2)-Fe(1)	57.67(4)	C(6)-Fe(4)-Te(6)	87.4(3)
Te(2)-Fe(2)-Fe(1)	58.38(4)	P(2)-Fe(4)-Te(6)	114.01(9)
C(3)-Fe(2)-Fe(3)	95.2(3)	Te(5)-Fe(4)-Te(6)	81.40(4)
Te(4)-Fe(2)-Fe(3)	54.40(4)	C(5)-Fe(4)-Fe(3)	89.6(3)
Te(3)-Fe(2)-Fe(3)	54.07(4)	C(6)-Fe(4)-Fe(3)	104.7(3)
Te(1)-Fe(2)-Fe(3)	151.71(6)	P(2)-Fe(4)-Fe(3)	161.71(10)
Te(2)-Fe(2)-Fe(3)	101.05(5)	Te(5)-Fe(4)-Fe(3)	58.48(4)
Fe(1)-Fe(2)-Fe(3)	146.09(6)	Te(6)-Fe(4)-Fe(3)	59.02(4)

Table S6 Selected distances ( $\text{\AA}$ ) and angles ( $^\circ$ ) for **5**.

<b>5</b>			
Te(1)-Fe(1)	2.6456(6)	Fe(1)-C(2)	1.741(5)
Te(2)-Fe(1)	2.6440(7)	Fe(1)-C(1)	1.749(5)
Fe(1)-P(2)	2.2785(14)	Fe(1)-P(1)	2.2784(14)
C(2)-Fe(1)-C(1)	94.7(2)	C(2)-Fe(1)-Te(2)	176.64(16)
C(2)-Fe(1)-P(1)	88.89(18)	C(1)-Fe(1)-Te(2)	88.16(16)
C(1)-Fe(1)-P(1)	93.38(16)	P(1)-Fe(1)-Te(2)	92.79(4)
C(2)-Fe(1)-P(2)	90.50(18)	P(2)-Fe(1)-Te(2)	87.61(4)
C(1)-Fe(1)-P(2)	90.79(16)	C(2)-Fe(1)-Te(1)	93.96(15)
P(1)-Fe(1)-P(2)	175.82(5)	C(1)-Fe(1)-Te(1)	171.30(16)
Te(2)-Fe(1)-Te(1)	83.268(19)	P(1)-Fe(1)-Te(1)	85.62(4)
P(2)-Fe(1)-Te(1)	90.29(4)		

Table S7 Selected distances ( $\text{\AA}$ ) and angles ( $^\circ$ ) for **6**.

<b>6</b>			
Fe(1)-C(1)	1.757(6)	Fe(1)-P(1)	2.2841(17)
Fe(1)-C(2)	1.762(7)	Fe(1)-Te(2)	2.6378(9)
Fe(1)-P(2)	2.2824(17)	Fe(1)-Te(1)	2.6489(8)
C(1)-Fe(1)-C(2)	94.5(3)	P(2)-Fe(1)-Te(2)	90.59(5)
C(1)-Fe(1)-P(2)	91.17(19)	P(1)-Fe(1)-Te(2)	87.57(5)

C(2)-Fe(1)-P(2)	89.57(19)	C(1)-Fe(1)-Te(1)	175.3(2)
C(1)-Fe(1)-P(1)	89.96(19)	C(2)-Fe(1)-Te(1)	90.12(19)
C(2)-Fe(1)-P(1)	92.13(19)	P(2)-Fe(1)-Te(1)	87.92(5)
P(2)-Fe(1)-P(1)	177.88(7)	P(1)-Fe(1)-Te(1)	90.81(5)
C(1)-Fe(1)-Te(2)	92.0(2)	Te(2)-Fe(1)-Te(1)	83.36(3)
C(2)-Fe(1)-Te(2)	173.46(19)	C(3)-Te(1)-Fe(1)	105.08(15)
C(9)-Te(2)-Fe(1)	107.02(16)		